

Review

Open Access



A review on high-performance flexible thermoelectrics: material, device, and applications

Abdul Basit¹, Jiwu Xin², Xin Li³, Tanveer Hussain⁴, Guoyu Wang⁵, Jiyan Y Dai⁶, Guangping Zheng¹

¹Department of Mechanical Engineering, The Hong Kong Polytechnic University, Kowloon 999077, Hong Kong, China.

²School of Electrical and Electronic Engineering, Nanyang Technological University, Singapore 639798, Singapore.

³State Key Laboratory of Material Processing and Die & Mould Technology, Huazhong University of Science and Technology, Wuhan 430074, Hubei, China.

⁴Department of Physics, Southern University of Science and Technology, Shenzhen 518055, Guangdong, China.

⁵College of Materials Science and Engineering, Chongqing University, Chongqing 400044, China.

⁶Department of Applied Physics, The Hong Kong Polytechnic University, Kowloon 999077, Hong Kong, China.

Correspondence to: Guoyu Wang, College of Materials Science and Engineering, Chongqing University, No.174, Shapingba Street, Chongqing 401331, China. E-mail: gywang2022@cqu.edu.cn; Jiyan Dai, Department of Applied Physics, The Hong Kong Polytechnic University, 11 Yuk Choi Road, Hung Hom, Kowloon 999077, Hong Kong, China. E-mail: jiyan.dai@polyu.edu.hk; Guangping Zheng, Department of Mechanical Engineering, The Hong Kong Polytechnic University, 11 Yuk Choi Road, Hung Hom, Kowloon 999077, Hong Kong, China. E-mail: g.zheng@polyu.edu.hk

How to cite this article: Basit, A.; Xin, J.; Li, X.; Hussain, T.; Wang, G.; Dai, J. Y.; Zheng, G. A review on high-performance flexible thermoelectrics: material, device, and applications. *Microstructures* 2025, 5, 2025028. <https://dx.doi.org/10.20517/microstructures.2024.56>

Received: 7 Jul 2024 **First Decision:** 14 Sep 2024 **Revised:** 25 Sep 2024 **Accepted:** 31 Oct 2024 **Published:** 18 Mar 2025

Academic Editor: Jun Chen, Zhigang Chen **Copy Editor:** Guomiao Wang **Production Editor:** Guomiao Wang

Abstract

Flexible thermoelectric (TE) materials and their devices have gained increasing attention due to the flexibility and lightness of flexible TE technology for low-temperature waste heat collection. In recent decades, various efforts have been devoted to the impressive efficiency of flexible TE technology including the synthesis, design, and integration of flexible TE generators. In this regard, the urgent need for eco-friendly, stable, and durable power sources motivates the booming market for integrated electronics. This review comprehensively summarizes the state-of-the-art development of flexible TE materials, device types, fabrication techniques, and the fundamentals behind their applications. In addition, the employed methods for moderate physical properties including theoretical analysis, experimental prospects, and importantly the challenges of flexible TEs are introduced. Moreover, we summarized the applications of flexible TEs in textiles, wearable electronics, waste heat utilization, and their applications in sensors, the Internet of Things, health monitoring, etc. We believe that this review addresses the current research challenges and their future directions to the researchers for choosing potential materials to explore flexible TE technology.



© The Author(s) 2025. **Open Access** This article is licensed under a Creative Commons Attribution 4.0 International License (<https://creativecommons.org/licenses/by/4.0/>), which permits unrestricted use, sharing, adaptation, distribution and reproduction in any medium or format, for any purpose, even commercially, as long as you give appropriate credit to the original author(s) and the source, provide a link to the Creative Commons license, and indicate if changes were made.



Keywords: Flexible thermoelectrics, sensors, devices, health-monitoring, human-machine interactions

INTRODUCTION

Recently, a dramatic escalation in the development of miniaturized and integrated devices for addressing urgent environmental issues has arisen due to the extinction of future fuels (coal, oil, natural gas, etc.) and the shift towards emission-free power sources^[1-4]. Herein, the advancement of energy technology and optimization of existing energy means attenuated severe energy crises resulting from their high consumption rate^[5]. In this aspect, thermoelectric (TE) technology assists the increasing demand for harvesting thermal energy and electricity, thus providing an environmentally benign route for power generation and refrigeration^[6]. Certainly, low-grade waste heats are the common energy sources, and their conversion efficiency to useful electrical energy in TE technology is known as dimensionless figure of merit $ZT = S^2 \sigma T / (\kappa_l + \kappa_e)$, where S , σ and T are Seebeck coefficient, electrical conductivity, and temperature, while κ_l and κ_e are the lattice and electronic thermal conductivity respectively^[7]. So far, a variety of strategies have demonstrated impressive improvements in power factors through band convergence^[8], band flattening^[9], and distortion of density of states^[9,10]; however, nanostructuring^[11] and hierarchical architecturing^[11] have resulted in suppressed thermal transports in mostly group IV-VI compounds, e.g., GeTe^[12], PbTe^[13], PbSe^[14], SnTe, etc^[15]. Additionally, excellent commercial applications in solid-state refrigeration^[16] by Bi₂Te₃ and SiGe^[17-19] turned into a diverse exploration of acceptable TE performance as evidenced by Slack's concept of "phonon-glass electron-crystal" (PGEC)^[20].

Current advances in solid-state physics are attributed to techniques such as symmetry-breaking, which have effectively manipulated TE performance through tuned band structures^[21]. However, these advancements are still hindered by challenges in carrier transport due to intrinsic vacancies^[22-25]. For instance, carrier and phonon transports were effectively realized in engineered GeTe by induced defects as shown in schematic Figure 1A. Similarly, domain structures featuring dislocations and vacancy clusters lead to easily broken metastable states and thus scattering sources in Ge_{0.97}Te [Figure 1B]. In addition, the replacement of foreign elements into nearby atoms significantly influences the transport, and hence moderate TE and mechanical properties were realized as shown in Figure 1C^[26]. For example, the transfer of charges was controlled via chemical bonding that resulted in various phenomena among charge transfer, structure, and physical properties of Y, Sb, Ag-doped GeTe. Ultimately, reduction in the Ge-Te-Ge bond angle leads to the charge transfer from Ge to Te, while doping of Sb and Ag leads to band convergence. In this regard, chemical bonding and coupling relationships through density functional theory reported the band sharpening at valence band maximum due to Y-doping at Ge sites that resulted in normalized transferred charge $\sim 0.23 e$ compared to pure GeTe $\sim 0.19 e$ ^[26].

Knowingly, electrical conducting and thermal insulating nature are essential for charge transport in TEs to realize energy conversion from interrelated scattering mechanisms of both charge carriers and phonons. For instance, Figure 1D demonstrates the scattering mechanisms including phonon-phonon scattering^[27], boundary scattering^[28], and impurities^[29]. So far, such strategies revealed that the internal microstructure of materials can be effectively controlled in nanotechnology; thus, enhanced phonon scattering leads to high performance^[30]. However, the transport of charge carriers is impeded by unmatched separation distances between scattering centers and electron/hole scattering. At last, theoretical observation for sub-devices shows a multitude of phonon resonances in the presence of nanopillars. Except for the above-mentioned phenomena of charge transport in solid-state materials^[31], flexible TEs play a crucial part of power generation in wearable electronics utilizing small temperature differences from the human body^[32-34]. Therefore, flexible organic and brittle inorganic thin film TE compounds have opened a new prospect of flexible TE technology^[35,36]. On the one hand, a variety of impressive flexible TE materials, including Ag₂S-based^[36-39] and AgCuSe-based materials, exhibited much higher power factors compared to organic TE

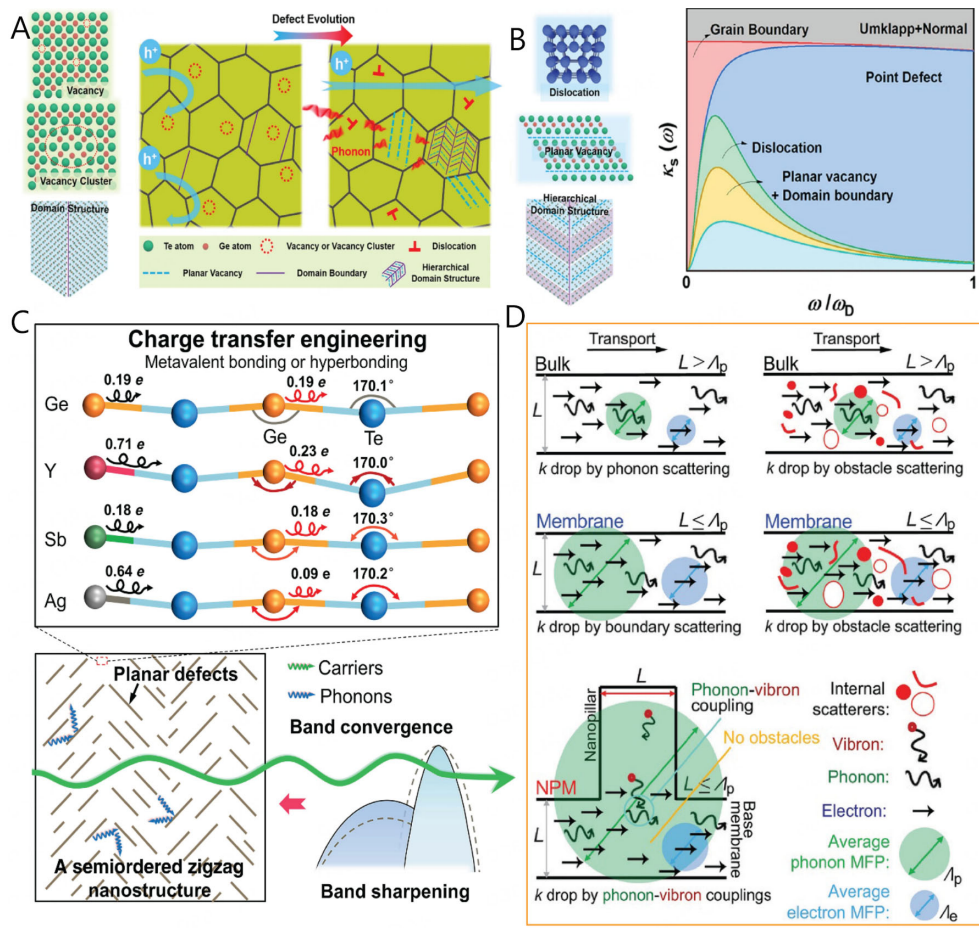


Figure 1. (A, B) Schematic illustration of the carriers and phonons in the presence of hierarchical structures, and the effect of various scattering mechanisms at 300 K^[50], Copyright 2022 Springer Nature. (C) schematic of the variation of bond angle, a semi-ordered zigzag nanostructure, energy band sharpening, and convergence by the charge transfer engineering^[26] Copyright 2023 Advancement of Science. (D) mechanisms revealing the reduction of thermal conductivity for TE conversion; bulk and reduced-dimension configurations, and NPM configuration respectively^[51]. Copyright 2023 Wiley-VCH GmbH. NPM: nanophononic metamaterial.

materials at room temperatures^[40,41], while on the other hand, high Seebeck coefficient in multifunctional flexible TE devices (TEDs) led to efficient sensing and power generation for thin sensors^[42]. Herein, remarkable power factors in flexible conductive polymers and carbon-based materials reveal the importance of Te-based flexible TE materials^[43,44]; thus, bismuth telluride-based alloys were proposed for flexible TE sensors and led to various applications in energy harvesting and overheating human body in sunlight^[45–47]. In this scenario, solid-state devices convert a temperature gradient into voltage^[48]; thus, flexible TEs can be utilized in widespread applications of sensors and wearable electronics for health monitoring^[49]. In this review, the above literature presents a better understanding of some recent flexible TEs, describing their characteristics and recently developed effective methods including analyses, high performance, experimental methods, challenges, etc. Also, the classification of flexible TEDs and their designs are detailed by comparing moderate and traditional flexible TEDs. Additionally, the last section summarizes widespread commercial applications and prospects of flexible TEs in detail.

STRATEGIES AND TYPES OF FLEXIBLE THERMOELECTRICS

To date, several portable devices are utilized for wearable applications and realizing communication and health monitoring, etc., while the unreliable capacity and lifetime of these devices hinder their large-scale

applications^[52]. Therefore, power supply systems for these wearable devices are ensured to be low-cost, highly efficient, durable, and sustainable TEDs that directly harvest low-grade human body heat and transfer the heat energy into electricity^[53,54]. For example, AgCu (Se, S, Te) solid solutions coupled with ductile material $\text{Ag}_{20}\text{S}_7\text{Te}_3$ have been made into a π -type flexible TED realizing an output voltage of 0.2 mV and power of 70 nW^[34]. Correspondingly, constructing a planer TED with inorganic TE materials exhibited inferior conversion efficiency due to poor thermal contacts in TED contacts^[55]; however, thin-film technology led to some bottom-up approaches and thus encountered the underlined lower cooling performance in mW self-powered nano-microelectronic devices, in contrast^[56–58]. Currently, thermal management of electronics and other industry applications are still limited, thus seeking challenging initiatives to design new approaches in future research of compatible integrated circuits (ICs)^[59]. Additionally, different crystallographic orientations exhibit surface atomic/electronic structures; thus, microstructure engineering results in desired physical and chemical properties; for example, higher anisotropy in chalcogenides might be controlled by microstructure that reveals improved flexibility of polycrystalline materials^[60]. Besides, the development of artificial intelligence is always demanded in flexible and wearable sensors for decoding a communication interface and transfer of information in human-machine interaction^[61–63]. In this regard, such sensors realize the conversion of applied external stimuli to detectable electrical signals via sensing mechanisms of piezoresistive^[64], piezoelectric^[65], and triboelectric^[66]. Additionally, a code by pressing a sensor can be sent to the device and thus highly secured information could be realized during human-machine interactions^[67], i.e., temperature^[68], magnetic field^[69], and humidity^[70]. On the other hand, some complex environments related to the human body including sweat, body heat, and sunlight have been focused in moderate wearable textiles through developed thermoelectricity^[71], photothermoelectricity, and piezoelectricity so far^[72]. Consequently, photothermoelectric textiles can convert photothermal heat to thermoelectricity and harvest waste heat from the human body and solar energy^[73]. Therefore, several flexible organic/inorganic hybrid photovoltaic devices have been prepared so far^[74,75]; however, their wide range of applications is limited by the instability factor.

In addition to the above approaches, flexibility and wearability were specifically considered for the comfortable attachment with human skin in wearable TEDs correspondingly^[76], e.g., organic/inorganic with poly(3,4-ethylenedioxythiophene) (PEDOT)-coated polypropylene fabrics and cotton fabric^[59]. Herein, organic or carbon-based TE materials have gained tremendous attention in TE fibers due to their impressive TE performance as compared to the organic materials^[77] through thermal drawing^[78] or coating on fiber to realize mechanical deformation such as stretching and twisting^[79]. Moreover, multifunctional photothermoelectric materials have attracted a great deal of attention due to their ability of heat-to-electricity conversion through photothermal and TE effects^[80], where traditional photothermoelectric materials lead to the conversion of light to heat and then to electricity, ultimately. For instance, TE films with strain-sensing performance ideally demonstrated a high Seebeck coefficient and hence electric voltage, while low thermal conductivity with stable temperature gradient and favorable flexibility make TE films more promising, i.e., conducting polymers^[81], inorganic crystalline semiconductors^[82], and carbon materials^[83]. In contrast, high thermal conductivity and low Seebeck coefficients restrict temperature sensitivity and output signals for strain-sensing devices; semiconducting chalcogenide glasses (ChGs) have been proposed thus demonstrating favorable for TE applications resulting from their low thermal conductivity^[84]. Besides, major challenges to the designing of self-powered temperature electronic skins (e-skins), organic TE materials, polypyrrole (PPy), and PEDOT^[85] have resulted in impressive flexibility and sensitivity in flexible substrates of polydimethylsiloxane (PDMS) and polyimide (PI)^[86]. Referring to the demanding applications with higher output voltage, wearable technology is still a core task for researchers due to unclear restrictions including bio-toxicity of inorganic TEs^[87] and unsatisfactory Seebeck coefficient in wearable organic devices^[88,89]. In this aspect, thermocells (TECs) have realized the generation of electronic

output mostly in lithium-ion cells^[90], metal-sulfur cells^[91], and metal-air cell^[91], though leakage and encapsulation are still challenging in TEC technology that could be resolved by integration of hydrogel electrolytes. Therefore, excellent mechanical properties with high stretchability and bendability in wearable devices could be attained. Herein, [Figure 2A](#) illustrates the number of papers published from 2000 to 2024 as retrieved from the Web of Science, where it is noticeable that the total number of published research on flexible TEs has been increasing since 2015 as compared to the other TEDs. Further, [Figure 2B](#) shows the graphical representation for various strategies utilizing flexible TEDs and their applications in textiles, wearable electronics, medical, robotics, industrial waste heat harvesters, human-machine interaction, etc.

Flexible thermoelectric textiles

Referring to the widespread applications of sensors in wearable electronics for health monitoring, [Figure 3A](#) demonstrates a schematic of the solid-state device harvesting temperature gradient into voltage via the Seebeck effect by body cooling/heating^[48,49]. Though wearable electronics are a poor option for many body management applications, flexible devices fabricated by embedded inorganics into flexible substrates were attracted towards textile fabrics, in contrast^[96,97]. For example, textile-based TEDs, created by laser printing of bulk inorganic TE legs, resulted in a textile substrate that was used in sportswear worn on the human wrist to measure circuit voltage [[Figure 3B, C](#)]. Interestingly, the indoor temperature (23 °C) has been experienced for both stationary and walking conditions^[98], suggesting that clothing fabrics could further be explored to utilize in textile-based TEDs for low-power wearable electronics applications.

In fabrics, the enhanced flexibility and TE performance with mechanical deformation led to research of stretchable inorganic TE material-based fabric; thus, stretchable inorganic TE textiles were proposed for monitoring the human body signals^[99]. Considering the importance of stretchability and stability of active textiles in TE fibers, stretchable Bi₂Te₃-based TE fabric was developed by Bi₂Te₃ nanoparticles (NPs) through chemical reduction method, leading to crack propagation tendency in these NPs as illustrated in [Figure 3D](#)^[100]. Referring to these durable NP networks, Bi₂Te₃ TE fabric resulted in stable electrical reliability under normal pressure ascribed by the governed broader areas between conductive fibers. [Figure 3E](#) illustrates current-voltage (I-V) curves varying under lateral strain and pressure^[101]; thus, higher electrical conductivity can be attributed to the broader contact areas between conductive fibers under normal pressure. Similarly, the reduction in band gap of Bi₂Te₃ NPs due to lateral strain attributes an increased electrical conductivity. Thereby, integrated wearable electronics with a sensing array feature high flexibility and stretchability in Bi₂Te₃ TE fabric as a black cotton fiber [[Figure 3F](#)]. These fibers could be utilized in the form of garments and thus pressure/temperature-sensing can be monitored on the mobile's screen with color pixels.

Referring to the optoelectronic properties, functional textiles have potentially been utilized in health, medical, and smart wear for reliable health management^[102]. In this aspect, green TE fabrics prepared by facile and carbon nanotube (CNT) electrospray on electrospun poly lactic acid (PLA) fabrics lead to durable devices that harvest energy and thus provide self-powered sensing performance [schematic [Figure 4A](#)]^[103]. With this novel technique, real-life wearable electricity generation from the human body as designed via integrated textile TE generators (TEGs) on a cotton wristband resulted in a generated voltage of 0.916 mV at room temperature. In addition, these TE fabrics demonstrated respiratory monitoring through a mask by observing the difference in breathing frequencies with recorded voltage signals [[Figure 4B](#)]. This effort elucidates that TE composite fabrics with moderate strategies could be explored and designed for high generated voltage; thus, healthcare can be realized in medical field.

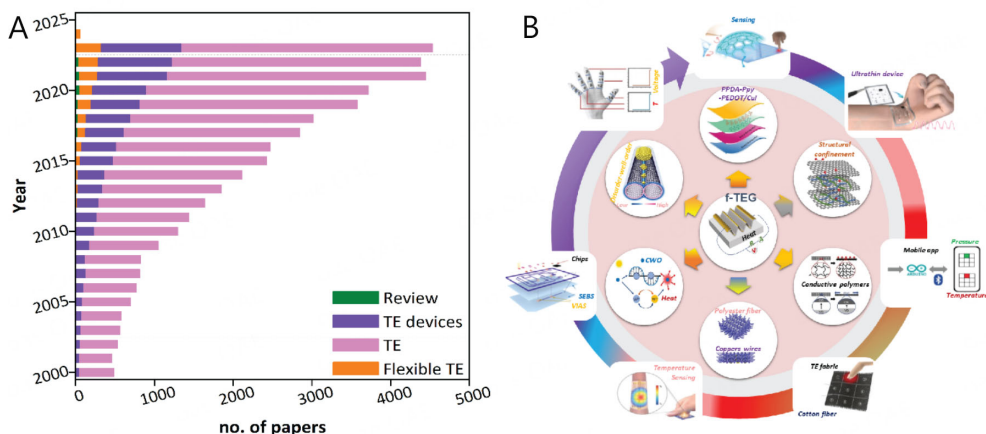


Figure 2. (A) Number of publications based on the thermoelectric technology research from 2000 to 2024 according to the Web of Science, and (B) graphical representation for distinguished strategies of flexible thermoelectric devices and their applications in textile, fabrics, sensing human-machine interaction, and robotics etc.^[10,92-95]. Copyright 2024 Springer Nature.

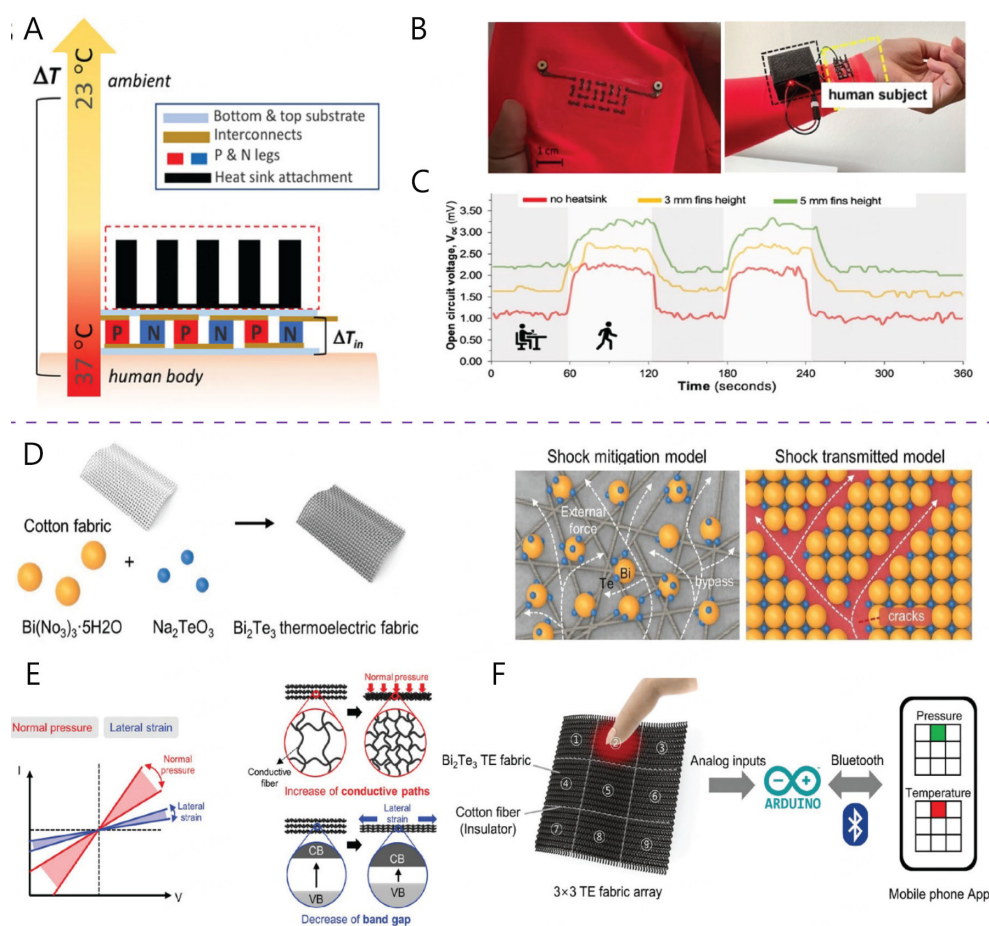


Figure 3. (A) Architecture of TE device for on-body applications representing a heat sink under vertical temperature gradient from the skin to ambient^[98], Copyright 2022 Wiley-CH GmbH (B) fabricated prototype and wearable wrist sleeve with textile-based TE device, (C) real-time measurement of open-circuit voltage output without a heat sink under stationary and walking scenarios^[98], Copyright 2022 Wiley-CH GmbH (D) representation of crack propagation tendency in NPs and bulk and SEM images of densely formed Bi_2Te_3 NPs inside TE fabric and (E, F) sensing mechanism of Bi_2Te_3 TE fabric and their illustration of the pressure and temperature-sensing array^[100]. Copyright 2023 Wiley-VCH GmbH. TE: Flexible thermoelectric; SEM: Scanning electron microscopy; NPs: nanoparticles.

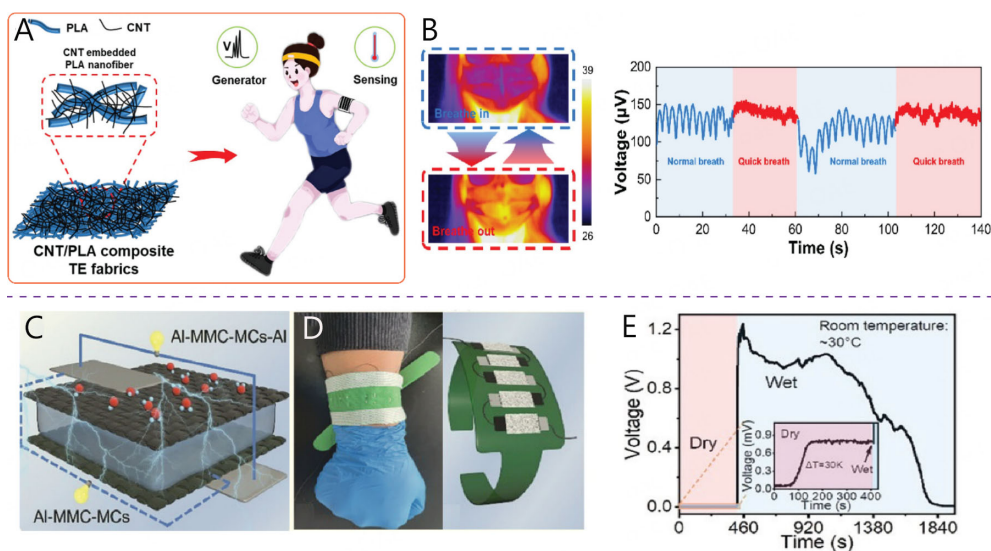


Figure 4. (A) Schematic of electrospay-on-electrospinning CNT/PLA TE composite fabric strategy^[103], Copyright 2023 Elsevier Ltd. (B) infrared images of ex-/inhalation of a volunteer wearing a mask with one unit of TE composite fabric and their detected voltage signal monitoring the normal breath and quick breath, (C, D) illustration of hydroelectric power generation with homogeneous and heterogeneous electrodes and a wristband assembled by five units of THEGs, and (E) performance of the MCs-MMC THEGs in dry and wet states^[107]. Copyright 2023 Wiley-VCH GmbH. CNT: carbon nanotube; PLA: poly lactic acid; TE: Flexible thermoelectric; THEGs: thermo-hydroelectric generators; MCs: MoS₂ carbonized silk; MMC: MoS₂/MXene-Cotton.

Currently, available wearable devices are mainly based on chemical fuels with recharging requirements; thus, thermoelectricity devices, such as nanocomposite and polycrystalline BiTe-based TEDs, were proposed, thus harvesting heat energy directly from the environment or human body based on the Seebeck effect^[104]. With this idea, increasing heat of the human body from mechanical energy was proposed to be utilized into affordable and sustainable electricity through smart wearable systems^[33]. Thus, the major application of hydroelectric generators (HEGs) is to take the water molecules and generate power through wearable electronics^[105]. For example, 2D transition metals, such as MoS₂, MXene, etc., have been proven to be potential candidates in fabrics^[106]. In this aspect, efficient flexible thermo-HEGs (THEGs) were developed between p-type MoS₂ carbonized silk (MCs) fabrics and n-type MoS₂/MXene-Cotton (MMC) fabrics [Figure 4C]^[107]. This effort reveals a hydrothermal method by a p-type conductor (1T-phase MoS₂ nanosheet on the surface of carbonized silk) facilitating multi-nanochannels and realizing the absorption of moisture. On the other hand, the n-type [van der Waals (vdW) heterojunctions of MoS₂ and MXene nanosheets] conductor facilitated a fast electron migration and thus led to power output. Such fabrication established a self-powered sensor, whereas a series of five devices as a wristband demonstrated a combined effect of sweat from the body surface during exercise. The MCs-MMC device further demonstrated an interesting TE effect in a dry atmosphere ultimately; hence, 0.825 mV thermal voltage output was obtained under a temperature difference of 30 K [Figure 4D, E]. This effort ensures the hydroelectric power generation capacity and suggests that sports clothes can be utilized for the installation of such devices and thus power generation can be realized. This work needs to be further explored through advanced fabrication that may lead to significant micropower supply in large-scale applications in the field of self-powered sensors and wearables.

Flexible thermoelectric electronics

Recent decades have witnessed considerable progress in the development of lightweight flexible electronic devices regarding their multiple varieties and fashion to the market^[108]. Many common energy supply devices are still heavy and present most flexibility concerns in wearable electronics; thus, flexible TEs electronics are emerging as a research hotspot^[109]. In this aspect, commercially available wearable fabrics-

based polymer TEs with low toxicity, adjustable structure, and excellent flexibility have gained huge attention recently^[110]. In addition to the challenges of device applications, excellent flexibility and output ability at the human body with fixed mechanical stiffness in advanced electronics are important^[111,112]. In TEs at a high range of temperatures, epitaxial growth plays a key role in controlling the anisotropy in crystals. However, conventional 2D epitaxial growth (films/nanocrystals) by vapor-phase deposition critically requires single-crystal substrates^[113]; therefore, 1D vdW epitaxial-growth in flexible single-wall CNT (SWCNT)-nanocrystal should play a potential role^[114]. Herein, the potential energy for a single atom on the surface of SWCNT features similar to SWCNT with higher potential energy in two SWCNTs and thus offers nucleation sites in nanocrystals [schematic Figure 5A]. For instance, (Bi, Sb)₂Te₃ nanocrystals present a well-established out-of-plane texture where closely packed high-symmetry orientations are aligned with SWCNT-bundle; however, tilt grain boundaries form between the consecutive nanocrystals and influence phonon transport of SWCNT-Bi_{0.5}Sb_{1.5}Te₃ hybrid ultimately [Figure 5B]. In addition, a prototype flexible micro-TED module (having ~650 nm-thick n-type and ~720 nm p-type counterparts) demonstrated a record high output power density of ~0.36 W cm⁻² at 30 K temperature difference, and hence a cooling power density ~92.5 W cm⁻² at ~400 K was realized in ICs [Figure 5C, D]. This effort provides a road map for the future moderation of thin-film TEDs in portable electronics via the development of nanoscale electrode printing technologies.

Turning to the generation of electricity from light and heat without greenhouse gas emissions, wearable solar TEGs (STEGs)^[115] have proved their importance; for instance, the commercial Bi₂Te₃ and Sb₂Te₃ TE legs led to a high output power of ~8.0 mW at a temperature difference of ~20 K^[116]. Major limitations of these materials including thermal impedance^[104] and regulating temperature for hot/cold surfaces were effectively encountered through the alternative photothermal materials as environmentally friendly and operative^[117]. Therefore, tailored molecular structured organic semiconductors^[118] and compatible plastic substrates^[119] were considered as the building blocks in photothermal materials for photoacoustic imaging^[120], solar desalination^[121], and photothermal-electric devices^[122]. In this aspect, high photothermal conversion efficiency (PCE) was attained from the absorption ultraviolet^[123] to near-infrared (NIR) region, especially the second NIR (NIR-II) region. Therefore, the incorporation of free radicals into films stabilizes photothermal radicals^[124]. In addition, organic functional materials were designed by co-crystal engineering by a facile approach, where electrospinning technology produced a controllable morphology and good stretchability in large-area nanofiber membranes^[125]. Flexible nanofibers may present an opportunity for a solar absorber layer, and may also lead to increased temperature gradient in wearable STEGs. Besides, electron donor tetramethylbenzidine (TMBD) and electron acceptor tetrachloro-benzoquinone (TCBQ) revealed the formation of organic photothermal co-crystals via a facile solution evaporation^[126]. The scalability and flexibility of these photothermal nanofiber membranes were attained via coating the CNT-based TE fibers thus resulting in a negative/positive value of voltage density without and with a TMBD-TCBQ (TTC)-polyurethane (PU) photothermal membrane, respectively [Figure 5E, F]. On the other hand, output voltage density for TTC-STEG with human skin contact was investigated through natural light, and a consistent voltage density variation in solar irradiance reflects that flexible and lightweight electronic devices can stably generate excellent TE power in wearable electronics.

Additionally, a variety of facile techniques for materials with diverse physical properties in micro/nanofibers resulted in a new generation of fibers beyond traditional optical fiber^[127,128]. For example, the Bi₂Te₃ and SnSe flexible TE fibers were attained by thermal drawing crystalline TE materials in a glass-fiber, whereas Bi₂Te₃ polycrystalline nanosheets revealed enhanced performance due to their preferential orientation during the fiber drawing process^[129,130]. Similarly, micro/nano TE fibers with Bi₂Te₃ core and borosilicate cladding resulted from the thermal drawing as shown schematically in Figure 6A. It can be seen that a stable interface

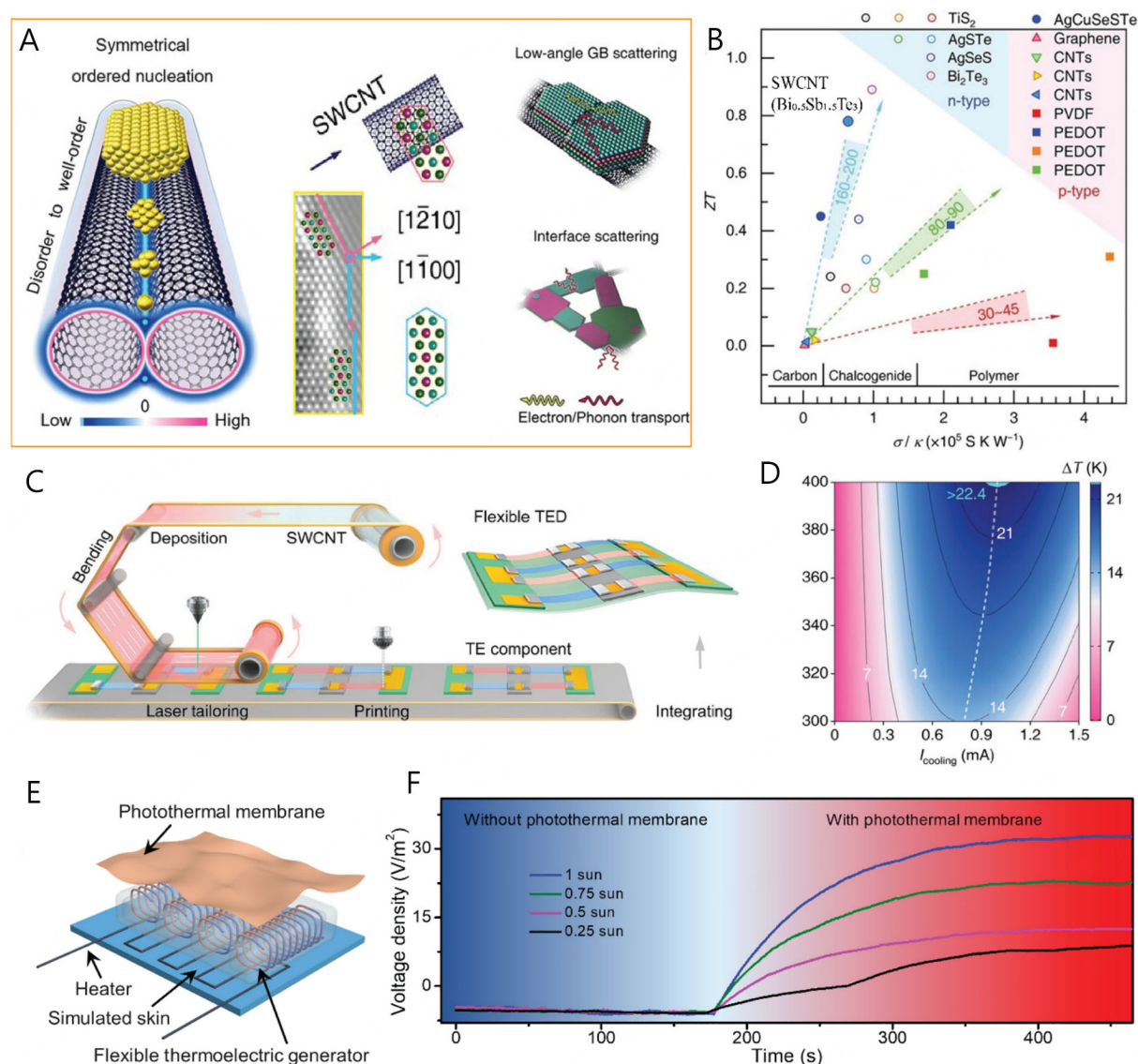


Figure 5. (A) Schematics of symmetrical nucleation from a disordered to a well-ordered arrangement and HRTEM of $(\text{Bi}, \text{Sb})_2\text{Te}_3$ nanocrystal illustrating highly-ordered SWCNT- $(\text{Bi}, \text{Sb})_2\text{Te}_3$ hybrids suggesting the carrier/phonon scattering by grain boundaries and interfaces^[114], Copyright 2023 Wiley-VCH GmbH (B) room-temperature ZT related to the σ and κ of flexible nanocarbon, chalcogenides, and SWCNT- $\text{Bi}_{0.5}\text{Sb}_{1.5}\text{Te}_3$ hybrid, (C, D) performance of the micro-TED module and measurement of cooling temperature as a function of applied cooling current^[114] Copyright 2023 Wiley-VCH GmbH and (E, F) schematics of TTC-STEG and their output voltage density under different light intensities^[126]. Copyright 2023 Advancement of Science. HRTEM: high resolution transmission electron microscopy; SWCNT: single-wall carbon nanotube; STEG: solar TEGs.

between glass cladding and Bi_2Te_3 core facilitates oriented nanosheet crystals in fiber cores^[131]. These fibers regulate the electrical transport with enabled interfacial engineering, and therefore efficient bending and lifetime are obtained. Herein, the stability of micro/nano TE fibers reflects further research on other TE fiber materials that may lead to the advancement in self-powered wearable electronics.

Besides, fabrics with combined photothermoelectric and hydroelectric properties suggest that some innovative and smart candidates realize efficient environmental energy. Such fabric converts light and heat energy into electric energy, while converting chemical energy of water molecules into electric energy (e.g., PEDOT-based photothermoelectric textiles)^[132]. Another effort revealed an increase in conversion efficiency

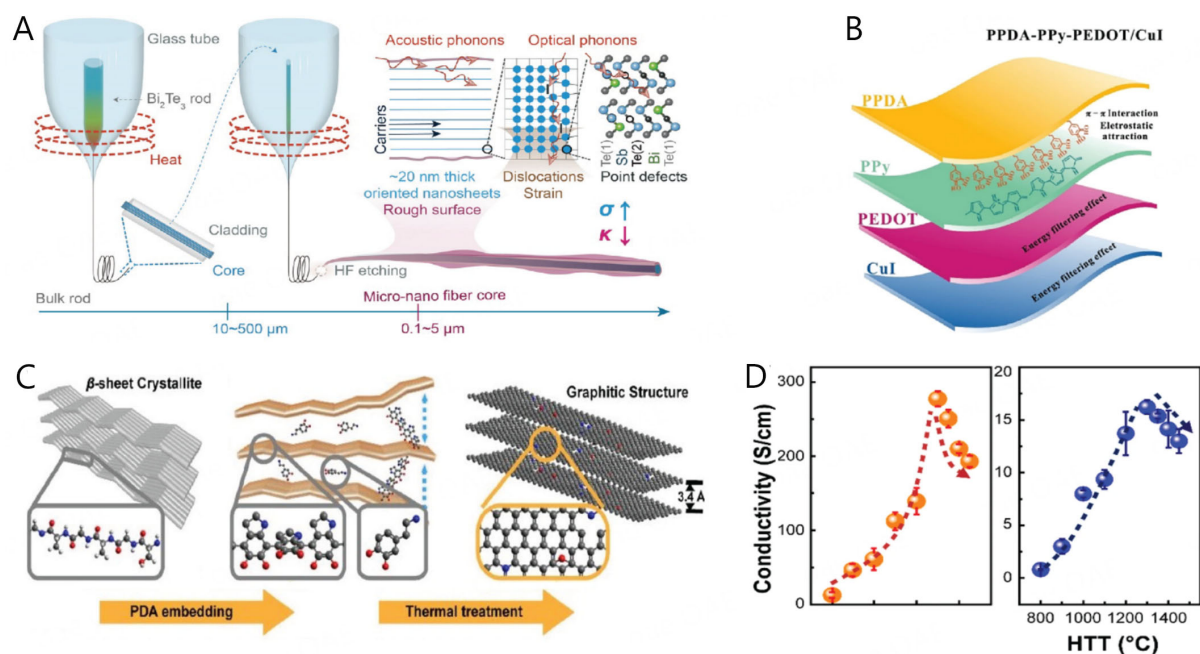


Figure 6. (A) Representation of micro/nano thermoelectric fiber prepared by the glass-fiber-template thermal drawing method, (B) drawing of the photothermoelectric yarn panel with wearing schematics and preparation process of PPDA-PPy-PEDOT/CuI photothermoelectric yarns^[94], Copyright 2023 American Chemical Society (C, D) illustration of delamination of silk fiber and the HTT-dependent conductivity of a single silk fiber and TPS fabrics^[10]. Copyright 2024 Springer Nature. PPy: polypyrrole; PEDOT: poly(3,4-ethylenedioxythiophene); TPS: thermally treated Polydopamine-embedded silks.

in wearable photothermoelectric yarn panels through photothermoelectric and hydrovoltaic effects [schematic Figure 6B]. Meanwhile, photothermoelectric p-phenylenediamine (PPDA)-PPy-PEDOT/CuI using organic/inorganic resulted in increased voltage output with a high-temperature difference. In this scenario, the thermal energy of the human body was collected due to the solar energy and body sweat^[94], and thus photothermoelectric and hydrovoltaic effect led to conversion capability into high Seebeck coefficient. Further, such phenomenon demonstrated an output of 41.19 mV in the infrared lamp with assembled photothermoelectric yarn PPDA-PPy-PEDOT/CuI, while on the other hand, synergistic photothermoelectric and hydrovoltaic on the human body resulted in increased voltage of 0.16 V under sunlight. Ultimately, this effort reveals that other organic/inorganic hybrids may be utilized for human body thermal energy, solar energy, and water energy in a broad prospect of wearable smart textiles.

Except for wearable textiles, the delamination of layered 2D compounds has attained great interest in electronic textiles including graphene and transition-metal dichalcogenides (TMDCs)^[133,134] due to their interesting features of stretchability and flexibility^[135]. Such characteristics result from weak strain which is inversely proportional to the thickness of a material and exhibit complex structure with amorphous chains, α -helix structures, and β -sheets in silk nanoribbons^[136]. As reported, the crystallites transform into graphitic structures even at high temperatures ~ 2300 °C leading to thermally robust electronic textiles for commercial silk^[137] and sensors^[138]. Figure 6C demonstrates a graphitic structure prepared after the intercalation of β -sheets in β -crystallites followed by heat treatment. Polydopamine (PDA) was considered to improve the ability of excellent adhesion of substrates including noble metals, oxides, semiconductors, ceramics, etc.^[139], however, the flexibility issue has always been a key parameter. The thermally treated PDA-embedded silks (TPS) reveal impressive flexibility and electrical performance by heat treatment temperature (HTT) ~ 900 °C^[137], and thus bring a possibility for TPS application operating under twisting and grabbing. The super

flexibility of the corresponding TPS suggests the potential use of thermally treated PDA-embedded wool and cotton^[10]. Similarly, the single fiber has been demonstrated to possess a high conductivity resulting from the inferior electrical contact fibers [Figure 6D]. This effort concludes that a single fiber with an advanced strategy may achieve high conductivity by tuning its electrical contacts and recommends that the corresponding fabric-based generator could be utilized in TE textiles.

Though smart wearable electronics are famous for motion monitoring in TEs, their designs are still challenging due to their ultrathin thickness; for example, 2D materials composed of graphene oxide (GO)^[140]. Nevertheless, the available layered microstructural backbone^[141] and polymer-based poly(ethylenedioxythiophene):poly (styrene sulfonate) (PEDOT:PSS) resulted in exceptional TE performance due to their additionally controlled oxidation level and hence high carrier concentration^[142]. Therefore, reduction treatment was proposed to enhance the TE performance in PEDOT:PSS incorporated into 2D GO, and hence modulation of carriers in reduced GO (rGO)/rPEDOT:PSS composite resulted in high TE performance^[143]. This approach elucidated that the effective alignment resulted in enhanced carrier mobility in rGO and thus ordered rPEDOT:PSS chains leading to the high efficiency of carriers^[144]. In addition to the mechanical flexibility of rGO/rPEDOT:PSS, a TE sensing glove demonstrated the device-level application by 14-micro TE sensors [Figure 7A], whereas rGO/rPEDOT:PSS films evaluated their TE ability by voltage signals from temperature difference with three common hand motions. This novel concept leads to the exploration of self-powered TE wearable sensors in many other TE materials in the field of precise recognition of human motions. Another work presents a solid-state device V_2O_5 -(rGO-1.5) reaching an ultimate Seebeck coefficient of $11.9 \pm 1 \text{ mV K}^{-1}$ demonstrating impressive thermal-electrical utilization for room temperature harvesting. This effort reveals the recorded value which is sufficiently higher than that of rGO, V_2O_5 , and V_2O_5 -(rGO-1.0)-based devices. In addition, external load further examines their stability and durability in energy conversion^[145]. Therefore, Figure 7B demonstrates that zinc ion thermal charging cells (ZTCCs) could be repetitive and long-term use at a temperature difference of $\sim 10 \text{ K}$ rather than a one-time energy source. These results reveal that the V_2O_5 -(rGO-1.0) solid-state might replace traditional batteries as a power source in health monitoring systems [Figure 7C].

Besides, the adaptability of both rigid and soft devices to human skin has enabled transformative electronic systems (TES) to demonstrate enhanced versatility in stretchable electronics^[146,147]. These TES designs consist of complex multilayer structures of flexible and stretchable electronics onto stiffness-tuned stimuli-responsive materials^[148,149]. Such an approach overcomes the limitations of layer integration, functionality, and inferior processors of large-scale devices. In a biological context, liquid metal gallium (Ga) has been proposed in TES applications with great mechanical tuning ability (9.8 GPa in solid-state)^[146,148], and suitable electrical property ($3.4 \times 10^6 \text{ Sm}^{-1}$)^[150]; thus, a phase change at functional temperature was attained. Interestingly, the phase transition of Ga (29.7°C) ensures wearable applications for TES. Therefore, stiffness-tunable gallium-copper (Ga-Cu) composite electronic ink was proposed, and the TES fabricated device revealed a temperature-dependent phase transition. Figure 7D reveals that stiffness enabled the tuned bidirectional feature for excellent TES functionality of the ultrathin epidermal photoplethysmography (PPG) device applied in the sensing of blood pulses. As reported, a double network of hydrogel contained ferro/ferricyanide, and stretchable polyacrylamide (PAAm)/SWCNT composite-hydrogel contained chloride/tin as a self-powered sensor for human motion^[31,151]. Nevertheless, flexible and stretchable TEDs, such as bamboo-like TEC fiber, emerge in hydrogel-based ionic TEC^[152]; however, PAAm hydrogel proposes microstructure of freeze-dried hydrogel with various interconnected reticular porous structures^[153]. Commercially, effective wearable hydrogel TEC devices for energy harvesting applications [Figure 7E], where the intrinsically stretchable TE hydrogels and carbon-based graphite paper are fabricated to realize a flexible and well-encapsulated device. In this regard, flexible and stretchable TECs

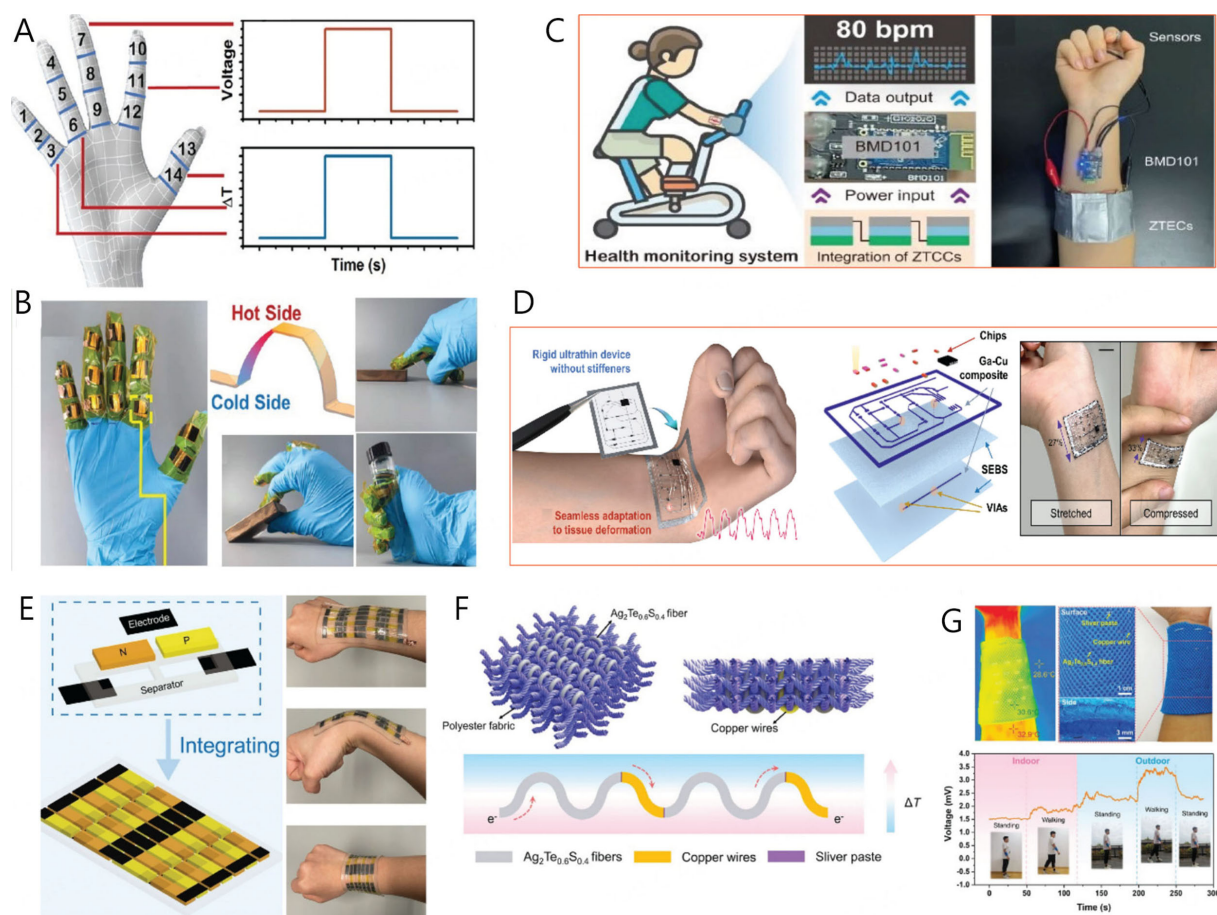


Figure 7. (A) Schematic device for precision recognition of complex motions such as TE sensors in knuckles and corresponding voltage signals, and (B) TE sensors on the glove and their sensing diagrams^[143]. Copyright 2022 Wiley-VCH GmbH (C) illustration for health monitoring system and body heat-charged health monitoring system^[145], Copyright 2023 Springer Nature (D) schematic of transformative handled PPG sensor and worn through rigid-soft mode conversion, an exploded-view of a transformative epidermal PPG sensor^[146], Copyright 2024 Advancement of Science (E) voltage-time curve of thermocell attached to the wrist during deformation, and (F, G) representation of the configuration of $\text{Ag}_2\text{Te}_{0.6}\text{S}_{0.4}$ fiber series in polyester textile, the temperature distribution by an infrared camera and monitoring on voltage output at standing or walking state^[155]. Copyright 2023 Wiley-VCH GmbH. TE: Flexible thermoelectric; PPG: photoplethysmography.

attached to the curved surface of human-arm may experience deformation and hence sensing applications could be realized.

Primarily, fiber-based TEDs are mostly composed of organic/inorganic hybrid fibers^[110]; however, some impressive inorganic TE fibers such as Bi_2Te_3 , SnSe , and PbTe fibers have been demonstrated to have high TE performance due to their narrow band gap and low thermal conductivity^[154]. In this regard, p-type $\text{Bi}_{0.5}\text{Sb}_{1.5}\text{Te}_3$ and n-type Bi_2Se_3 fibers generated an output voltage of 5 mV at temperature gradient $\Delta T=8\text{ K}$ ^[78], while Bi_2Te_3 -based TED resulted in $\sim 0.47\text{ mW}$ under $\Delta T=19\text{ K}$ ^[130]. Further, the intrinsic rigidity of inorganic materials results in a weak tensile strain of TE fibers and thus limited mechanical freedom. Herein, the limited flexibility of such devices to attach them with curved surfaces compromises their applications largely in wearables. On the other hand, combining the inorganic fillers into the organic host, inorganic $\text{Ag}_2\text{Te}_{0.6}\text{S}_{0.4}$ fibers through the direct preform-drawing method resulted in super flexibility for the first time with a substantial Seebeck coefficient of $82\text{ }\mu\text{VK}$ ^[155]. Therefore, the impressive TE performance of $\text{Ag}_2\text{Te}_{0.6}\text{S}_{0.4}$ fiber allows for potential application in wearable electronics such as $\text{Ag}_2\text{Te}_{0.6}\text{S}_{0.4}$ fibers resulting in an output

voltage of 1.5 mV and 2.5 mV at a temperature difference of 2.3 K in indoor and outdoor environments, respectively [Figure 7F, G].

Flexible thermoelectric organics/inorganics

Organic conducting polymers such as PEDOT, poly(3-hexylthiophene-2,5-diyl) (P3HT), and polyaniline (PANI) are considered natural candidates presenting excellent TE performance and flexibility due to their inherited bendable and ductile mechanical features^[156,157]. While considering their inferior mobilities ($\sim 1 \text{ cm}^2 \text{ V}^{-1} \text{ s}^{-1}$), power factors are limited as compared to the classic brittle inorganics $\sim 20 \mu\text{W cm}^{-1} \text{ K}^{-2}$ near room temperatures^[158,159]. Likewise, some recent studies of ductile inorganic candidates were highly appreciated in thermoelectricity due to their impressive flexible mechanical performance similar to those of classic inorganic materials, e.g., Ag_2S -based compounds^[35,41,160]. Room-temperature Ag_2S possesses a ductile nature and reveals a very low ZT of about 44 at 300 K^[41], while alloying Se/Te led the Ag_2S -based n-type ductile inorganic TE compounds leads to a high ZT 0.45 at 300 K^[161–163]. Except for a great development in present inorganic TE materials, classic Bi_2Te_3 and Ag_2Se -based materials are still unmatched to these present organic materials to challenge the power output and flexible applications^[164–166]. Thereby, morphotropic phase boundary (MPB) was studied as a transition region in phase diagram that separates two phases with different crystallographic symmetries in TEs owing to their lack of material competing phases^[167,168]. For example, $\text{Ag}_2(\text{Se}, \text{S})$ -based compounds revealed a change in crystal structure from orthorhombic to monoclinic as S content increased and led to phase boundary that affected corresponding chemical properties^[41,169]. These boundaries were tuned through adjusting heat treatment in orthorhombic $\text{Ag}_2\text{Se}_{1-x}\text{S}_x$ pseudobinary materials and thus MPB sufficiently integrates the features of high TE performance of ZT ~ 0.61 at room temperature^[170]. Further, a flexible in-plane TED with superior normalized material exhibits a maximum power density reaching 0.26 W m^{-1} under 20 K. Figure 8A presents the pseudobinary phase-diagram at 300 K to 480 K for Ag_2Se - Ag_2S , where the separated phase boundary by different heating process are presented (for x larger than 0.4 smaller than 0.2). Therefore, orthorhombic-monoclinic transition temperature decreases with increasing x owing to phase boundaries with reported MPB for lead zirconate titanate (PZT) phases^[171]. In addition, these ductile materials around MPB result in high TE performance as the flexible in-plane device $\text{Ag}_2\text{Se}_{0.67}\text{S}_{0.33}$ (n-type leg) and Pt-Rh wires (p-type leg) device have a high normalized power density of $\sim 0.26 \text{ W m}^{-1}$ at $\sim 20 \text{ K}$ [Figure 8B, C]. However, the resulting value is almost three times higher than that of the $\text{Ag}_2\text{Se}_{0.5}\text{S}_{0.5}$ /Pt-Rh device under the same conditions^[81,172–175]. This work summarizes that MPB in other ductile materials may be explored by modulating the pseudobinary phases, which gives rise to the high normalized power density and durability as compared to the classical Ag_2Se and Bi_2Te_3 -based materials.

Additionally, 2D vdW crystals, including InSe, MoS_2 , SnSe_2 , GaSe, etc., also demonstrated good ductility similar to metals near room temperature^[160,176]. However, alloying and elemental doping have realized a maximum power factor in a bulk single crystal of $\text{SnSe}_{1.95}\text{Br}_{0.05}$ near $\sim 10.8 \mu\text{W cm}^{-1} \text{ K}^{-2}$ at 375 K as higher than that of Ag_2S -based and AgCuSe -based plastic TEs. Similarly, bulk SnSe_2 -based crystals realize high power factors such as classic brittle TE materials by synthetic conditions leading to modified stacking in different polymorph crystal structures [Figure 8D, E]^[160]. This work suggests that Sn and Se atoms in three adjacent [Se-Sn-Se] triatomic layers are slightly staggered with available dark points in vdW. Meanwhile, the formation of stacking polymorph SnSe_2 2D vdW crystals was tuned by Cl/Br dopants and resulted in increased carrier mobilities and carrier concentrations. Additionally, 2D vdW SnSe_2 -based single crystals resulted in a record high normalized high power density of $\sim 0.18 \text{ W m}^{-1}$ at a temperature difference of $\sim 30 \text{ K}$ [see Figure 8F]. This effort implies that other plastic or ductile TE compounds can be studied along with the optimization of 2D vdW materials for practical application in flexible TEs.

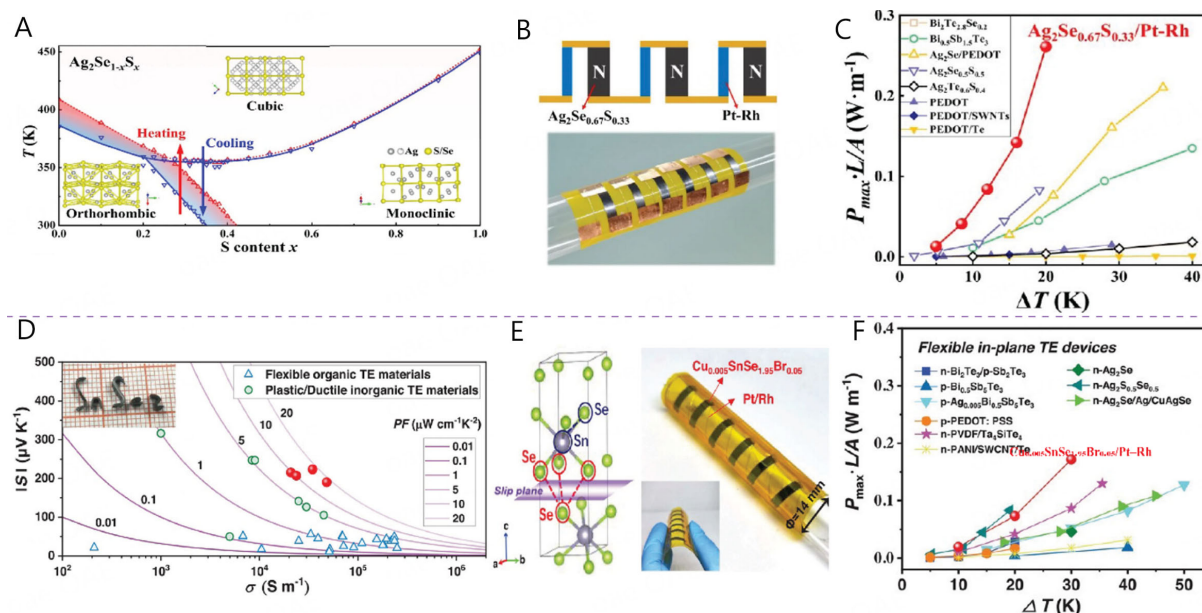


Figure 8. (A) $\text{Ag}_2\text{Se}-\text{Ag}_2\text{S}$ phase diagram based on the heat flow curves (schematics of the cation Se/S framework in orthorhombic, monoclinic, and cubic structures)^[170]. Copyright 2023 Springer Nature (B, C) optical image and comparison of the normalized maximum power densities of the materials among $\text{Ag}_2\text{Se}_{1-x}\text{S}_x$ -based inorganic, inorganic-organic hybrid flexible, and organic flexible TE devices, (D) room-temperature absolute value of Seebeck coefficient as a function of electrical conductivity for plastic/ductile bulk SnSe_2 -based crystals (red spheres), and other reports for comparison, (E, F) optical images of a six-couple flexible $\text{Cu}_{0.005}\text{SnSe}_{1.95}\text{Br}_{0.05}/\text{Pt-Rh}$ in-plane TE device with $\text{Cu}_{0.005}\text{SnSe}_{1.95}\text{Br}_{0.05}$ as n-type legs and Pt-Rh wire, and comparison of normalized maximum power density among the reported flexible in-plane TE devices^[160]. Copyright 2023 Wiley-VCH GmbH. TE: Flexible thermoelectric.

Besides, polymer TEs with low toxicity, adjustable structure, and excellent flexibility have gained huge attention recently^[110]. Herein, conducting polymers poly(3,4-ethylene dioxythiophene):poly(styrene sulfonate) (PEDOT:PSS) have demonstrated high-performance thermoelectricity attributed to their high conductivity and water-processibility. Inorganic TE fillers have been incorporated into PEDOT:PSS, and resulted in enhanced Seebeck coefficient; however, some nanoscale fillers including CNTs, graphene, and bismuth telluride particles exhibited the modulation of interfacial energy barrier between heterogeneous phases^[177]. In contrast, the distribution of NPs in polymers facilitates tuned electronic pathways and thus optimizes the transport properties, while high-quality composite TE fibers may not produce organic/inorganic composites in films due to their uniform dispersion in polymeric environments. In this aspect, PEDOT:PSS/Te composite TE fibers were proposed through wet spinning; thus, interfaces with different energy barriers facilitated optimized Seebeck coefficient. In addition, the corresponding interfacial energetic mismatch of ~ 0.10 eV in PEDOT:PSS/Te composite fibers results in effective carrier transport and thus a high power factor of $\sim 233.5 \mu\text{W m}^{-1}\text{K}^{-2}$ ^[108]. Correspondingly, the produced PEDOT:PSS/60 wt% Te composite fiber TEG coated with silver paste demonstrated higher sensitivity even at low-temperature stimuli as compared to other wearable sensors such as PEDOT:PSS/CNT/waterborne PU [Figure 9A, B]. Further, the attached sensor to robotic fingers demonstrated smart detection even at a wide range of temperatures and realized water heating and cooling by providing thermovoltage across the fiber [Figure 9C, D].

Tremendous attention has been paid to the conjugated polymer composites and realized impressive performances, though major use in practical applications is restricted by their energetic disorder and hence inferior charge transport. For example, low energetic disorder and amorphous conjugated polymers (planar backbone) were utilized in many applications of field-effect transistors and TEs^[178,179]. Generally, polymers

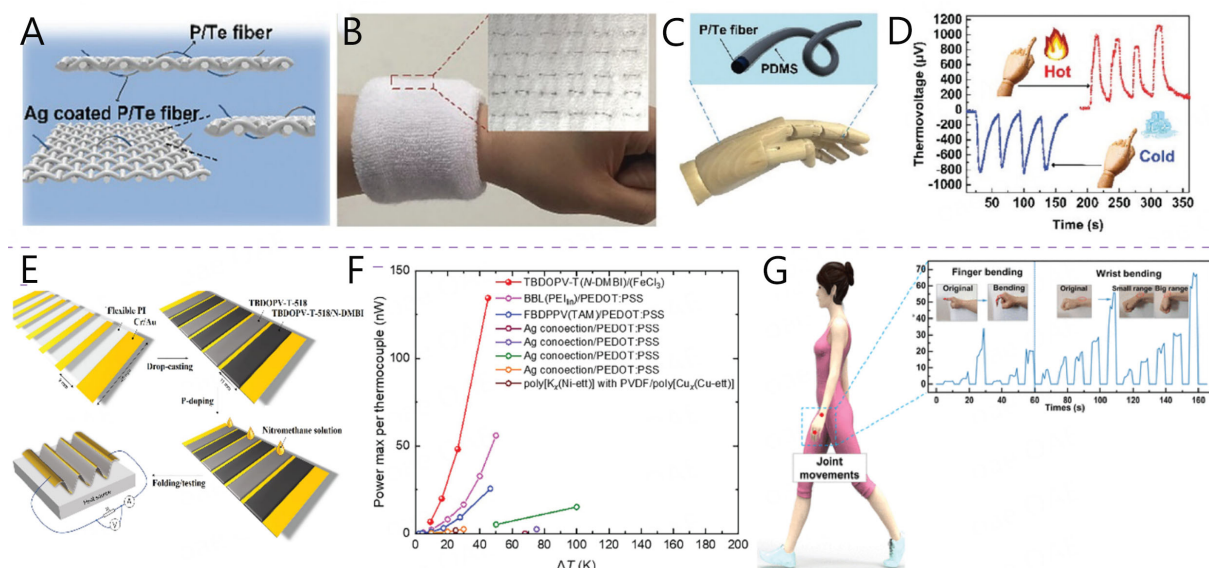


Figure 9. (A, B) Thermoelectric fiber and schematic illustration of the working principle of TE fabric^[108], Copyright 2024 Wiley-VCH GmbH (C, D) schematic of a prototype fibrous self-powered temperature sensor and its corresponding thermovoltage signals by heating and cooling, (E, F) fabrication and testing of single-polymer flexible TEG, and comparison of reported power output per module of polymer TEGs, and (g) representation of bending at joint and their real-time response of the sensor^[187]. Copyright 2024 American Chemical Society. TE: Flexible thermoelectric; TEGs: TE generators.

are not often crystalline and possess high carrier mobilities; thus, the concept of mobility has triggered their applications in TEs^[180-182]. This observation leads to a pathway to optimize n-type electrical performance in weak-crystalline rigid rod-conjugated polymer based on thiophene benzodifurandione oligo (*p*-phenylenevinylene) (TBDOPV) with a high conductivity of $\sim 100 \text{ Scm}^{-1}$ and a power factor of $\sim 200 \mu\text{Wm}^{-1} \text{ K}^{-2}$ ^[183,184]. Further, a flexible organic TEG was developed from doped TBDOPV-T-518 (n-type and p-type) and PI film [Figure 9E]^[185], and the power output per thermocouple was fifty times higher than other reports for polymer TEGs was demonstrated as shown in Figure 9F^[186]. In addition, the composite electrodes are used as flexible films, touch monitors, and flexible sensors. Thus, advancements in the accessories for smart wearables, including e-skins, smart fabrics, and electronic flexible sensor devices, continue to emerge due to their features such as ultrathin design, portability, waterproofing, and breathability. For instance, the utilization of composite electrodes in flexible resistive strain sensors was proposed to detect human motion [Figure 9G] with the experience of change in resistance by strain in different parts (e.g., bending of fingers and wrist)^[187]. Ultimately, it elucidates that TECs made of hydrogel might harvest low-grade heat (such as body heat) to a potential difference. Also, soft and stretchable TEC devices are needed to fabricate that may replace wearable electronics or health sensors by effective methods and geometrical design of the device.

APPLICATIONS OF FLEXIBLE TE TECHNOLOGY

Flexible thermoelectrics in health-monitoring

Referring to the above ideas, photothermal nanomaterials of metals^[188], inorganic semiconductors^[189], and polymers^[190] have received increasing attention to the potential solar-to-thermal efficiency in solar TEDs for output power. For example, a rationally designed CNT flexible wood membrane in a 300-1200 nm region revealed a high solar thermal efficiency of $\sim 81\%$ ^[191]. However, absorption of these materials in the 380-780 nm spectrum led to the challenging dark manifestation^[192]. In this regard, the NIR region experiences the highest proportion of $\sim 52\%$ of solar energy which may contribute to high thermal effect through effective absorption and hence conversion of solar light^[193]. Another report reveals that tungsten bronze nanomaterials lead to the absorption of NIR light and high visible transmittance, and thus high

photothermal conversion in some wearable electronics^[194–196]. With this approach, Cs_xWO_3 (CWO) NPs have demonstrated impressive photothermal conversion, and based on these NPs CWO@PU nanofiber membrane by electrospinning resulted in great stability with a generated voltage of ~ 234 mV at a temperature gradient ~ 10 K [Figure 10A]^[197]. Additionally, impressive NIR absorption of CWO-NPs makes the CWO@PU photothermal membrane a stable solar-thermal harvester working on the human arm and resulting in an output voltage in sunlight [Figure 10B]. This approach indicates that CWO@PU photothermal membranes may be useful for other wearable electronic applications.

In search of stretchable TE materials, flexible devices for energy generation are wearable health monitors, triboelectric nanogenerators, etc.; among them, hydrogels demonstrate remarkable ductility, and intrinsic properties to attain large-scale strains in human soft tissues^[198]. Generally, conventional hydrogels are considered unfavorable due to their inferior conductive properties that restrict large-scale applications in electronics and sensors^[199,200], i.e., conductive hydrogels (electronic conductive and ionic conductive hydrogels)^[201,202]. Familiar with the promising harvesting strategy of photothermal conversion, introducing photothermal agents into a hydrogel matrix leads to various morphological changes as light-triggered with increased local temperature, which can be utilized in cancer therapy, tissue repair, and sensors^[203,204]. In this aspect, photothermal agents with NIR absorbance based on two-dimensional transition metal carbides such as MXene emerge in a variety of applications, i.e., catalysts, batteries, photothermal therapy, and sensing. In contrast, MXene as a suitable material was proposed to fabricate a conductive hydrogel and realize photothermal conversion property. Herein, electronic and ionic conductive (KMGHCA) hydrogel with high stretchability was prepared using an integrated two-dimensional MXene ($\text{Ti}_3\text{C}_2\text{T}_x$) nanosheet in a poly(*N*-hydroxyethyl acrylate) matrix [Figure 10C]^[205]. Thus, KMGHCA hydrogel leads to impressive strain sensitivity of human motion [schematic Figure 10D]. Such personalized health monitoring can further be explored with self-powered triboelectric nanogenerators.

Referring to the vigorous development in artificial intelligence, wearable TEDs emerged in intellectualized sensors that potentially serve the human body as a sustainable bioenergy source for powering wearable electronics^[206]. Familiar information related to body/skin temperature, i.e., intestinal flora and metabolite levels^[207], allergies^[208], and arthritis^[209], can be monitored quantitatively by wearable electronics (stretchable joint sensors). In this aspect, a flexible fabric/PEDOT:PSS strain sensor on the elastic bandage experiences deformation in a transverse direction under longitudinal stretching and thus fiber bundles possibly come into contact as shown in Figure 10E^[44]. Upon contact, stretched fabric on the joint governs conductive pathways regarding environment temperature, and thus DC and AC components (V_1 , V_2) of flexible TEG extracted the locomotion speed and skin temperature accordingly [Figure 10F]. In this way, wearable sensing electronics can monitor various characteristics related to the motion of a human body, and thus realize the effective solution to healthcare.

Flexible thermoelectrics in sensing

Turning to the huge emergence of flexible electronics, many applications have potentially been acknowledged such as health monitoring, bionic e-skin, and robotic sensing with the human sensory ability of stimuli, e.g., pressure, strain, temperature, etc.^[210,211]. In this regard, stretchable sensing platforms based on human motion were proposed to monitor physiological conditions over shape transformation^[212]. These detections were made by self-powered electronic devices relaying on piezoelectric, electrostatic, or triboelectric mechanisms^[213,214]. However, flexible resistive tactile sensors emerged due to their high performance, simple design, adjustable sensitivity, and detection range^[215]. Recently, a fibrous mat prepared by electrospinning and *in situ* polymerization growth of PU microfibers and thus multi-walled CNTs (MWCNTs) were grown on a layer of PEDOT [Figure 11A]^[93]. In this aspect, MWCNTs were embedded into PU and thus facilitated conductive paths. However, the interactions between MWCNTs and PEDOT

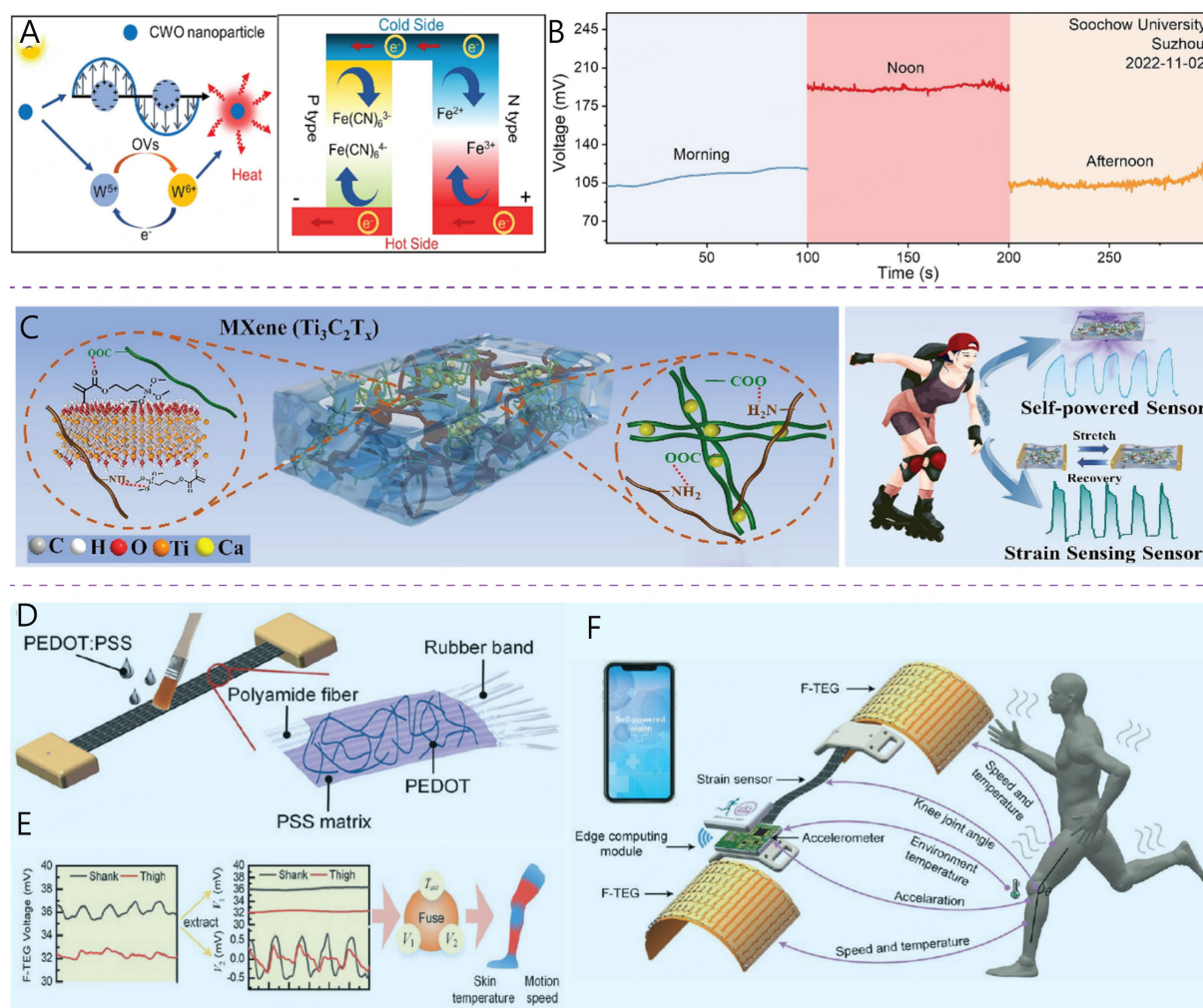


Figure 10. (A) Photothermal conversion mechanism of $\text{Cs}_{0.32}\text{WO}_3$ and their corresponding configuration and working mechanism of a TEG device^[197], Copyright 2023 Elsevier B.V. (B) open-circuit voltages of CWO-TEG worn on the arm in morning, noon, and afternoon, (C, D) representation of the chemical structures for the development of KMGHCa gel and their applications in sensing base, (E, F) 3D structure of the wearable system that enables comprehensive motion monitoring through a synergistic fusion of f-TEGs, a strain sensor, and an accelerometer, and computing framework for analyzing skin-temperature, locomotion and metabolic energy^[44]. Copyright 2023 Wiley-VCH GmbH. TEGs: TE generators; CWO: Cs_xWO_3 .

sheets result in pressed contact points between PEDOT/MWCNT@PU mat and electrodes upon pressure. Interestingly, pressure sensors based on PEDOT/WMCNT@PU mat have attracted great attention in applications including human physiological signal monitoring. For example, the sensor adhered to the mask and recorded the respiratory process due to the low pressure induced by different states of deep and normal breathing [Figure 11B]. Similarly, the attached sensor to the neck detects the carotid pulse, and thus, a carotid pulse rate of 81 beats per minute was recorded in good agreement with the heart rate test. Such high-precision properties in pulse-waveform analysis can further be explored for health monitoring.

Turning to stretchable TE self-powered sensors as wearable electronic devices, their challenging parameters were further investigated in PEDOT/MWCNT-based TE fabrics^[216]. These fabrics for self-powered strain-temperature sensing were prepared through spray combined with *in situ* bio-polymerization, featuring the energy-filtration effect of PEDOT and MWCNT that leads to enhanced TE performance in fabrics. Further, PEDOT/MWCNT-based TE fabrics demonstrated great stretchability after 2,000 repetitive stretching cycles

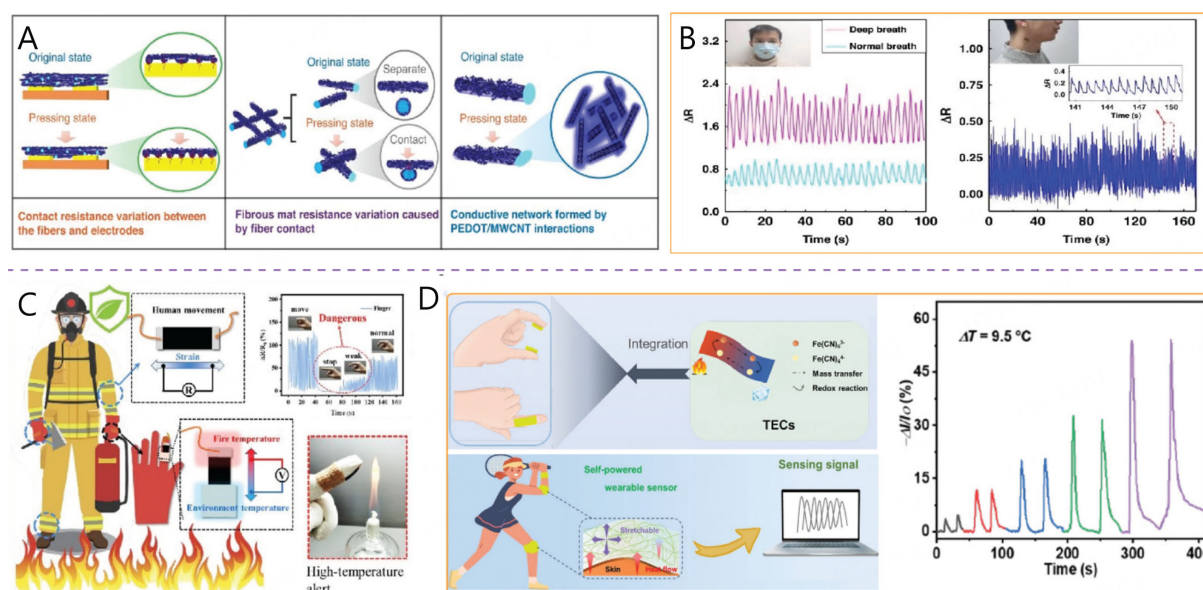


Figure 11. (A) Resistance variation between the fibers and electrodes, fibrous mat, and PEDOT/MWCNT interactions, and (B) respiratory monitoring under breathing, and carotid pulse monitoring^[93]. Copyright 2023 Springer Nature (C) schematic of fabric-based strain-temperature PEDOT/MWCNT@PLF sensor for health anomaly upon finger, wrist, and ankle joint and physical wearing of the glove in high-temperature^[92], Copyright 2023 Springer Nature (D) TEC packaging, and conceptual application of BC organogel-based electrolyte and voltage-time curves of BC organogel-based TECs with corresponding variation signals upon movement^[224]. Copyright 2023 Wiley-VCH GmbH. PEDOT: poly(3,4-ethylenedioxythiophene); MWCNT: multi-walled; PLF: polyester-latex mesh fabric; CNTs: carbon nanotube; TECs: thermocells.

that recommend PEDOT/MWCNT@PLF strain sensors for integrated clothing/accessories of human health monitoring. On the other hand, dual-mode integrated sensors to the wrist, fingers, knees, and ankles can detect motion in real-time, and further, the real-time electrical resistance retorts the sensors for joint movements and signal recording [Figure 11C]. Additionally, the smart glove of PEDOT/MWCNT tends to sense a temperature difference between body and flame temperature if near the flame by an output of thermal voltage signal. These synergistic-mode temperature/strain sensors may have great potential in medical and healthcare applications to control high-risk and child care.

With the continuous development of flexible wearable electronics, electricity power sources are highly demanded^[217], such as piezoelectrics^[218], TEGs, etc^[219]. However, thermoelectrochemical cells (TECs) have aroused great interest due to their conversion ability of low-grade heat < 100 °C to electricity by thermogalvanic effect^[220]. These devices generate a large Seebeck coefficient due to the potential difference between redox couples; for example, redox species such as $\text{Fe}^{[5]}_6^{4-}/\text{Fe}^{[5]}_6^{3-}$ possess higher Seebeck coefficient than $\text{Fe}^{2+}/\text{Fe}^{3+}$ (1.4 mV K⁻¹ and 1.0 mV K⁻¹, respectively). It has been noted that the temperature gradient between the human body and environment attributes a constant dragging force in TECs that is unprecedented for wearable electronic technology in a long-time power supply^[85]. A series of efforts revealed the attraction of gel-based electrolytes in comparison to liquid-base wearable devices^[221,222]; therefore, bacterial cellulose (BC) was influenced greatly as a natural hydrogel owing to its green and low toxic nature combined with great flexibility and biocompatibility^[223]. Besides some favorable mechanical properties and available intrinsic nanochannels of nanofibers, natural BC hydrogel fibers favor excellent ionic conductivity as compared to polyvinyl alcohol (PVA), PAAm, etc. Herein, BC hydrogel in the electrolyte matrix of TECs was proposed with a redox couple of $\text{K}_4\text{Fe}^{[5]}_6/\text{K}_3\text{Fe}^{[5]}_6$ ^[224]. This approach resulted in significant TE performance due to the increased Seebeck coefficient from crystallization of $\text{K}_4\text{Fe}^{[5]}_6$ and thus leading to self-powered sensors of BC organogel-based TECs [Figure 11D]^[224]. In this regard, TEC

resulted in a consistent output voltage upon being bent, stretched, and compressed, suggesting the reaction of TEC against multidimensional deformation as inherited by BC hydrogel may lead to potential utilization in wearable devices. This effort demonstrates a strain sensing from skin heat at joints with wearable BC organogel TECs, while mechanical features led to integrated BC organogel-based electrolyte to bending of finger. In addition, bending activity was detected with a self-powered strain sensor and their corresponding current variation signals, suggesting the increase and decrease of resistance upon releasing the bending of the finger. Such flexible strain sensors with BC organogel-based TECs can further be explored to utilize in other physical detection self-charging wearable electronics.

Sensing recognition in multifunctional materials could be synergetically boosted to be utilized in effective fire warnings. Literature reveals that deep learning can further be used for data optimization and processing due to its capability of deep feature extraction, and thus signal classification can be obtained^[225]. In this regard, the smart fire source sensing system demonstrated impressive output voltage and response time in a single-walled CNT/P3HT (SWCNT/P3HT) flexible composite^[226]. Herein, the power factor of P3HT/SWCNT increases by up to 97%, recommending P3HT/SWCNT composite for device fabrication. Additionally, holes/electrons were attributed to the separation between the donor (P3HT) and acceptor (SWCNT); thus, non-equilibrium electron/hole migrated to the dark end. Further, temperature difference and light-dark contrast simultaneously resulted in illumination upon light-induced heat. Moreover, a comparison of both TE and photoelectric modulated sensors (SWCNT/P3HT composite film) is presented in Figure 12A, where an improved effect is recorded for resultant output voltage and time in comparison light and heat alone as larger than the value recorded under heating alone. However, rapid reduction in output voltage would occur due to the removal of concurrent stimulus; therefore, SWCNT/P3HT-incorporated composite may further be utilized in circuit microcontrollers for smart fire source sensing devices and human protection against hazards.

Despite the current realization, the complex application scenarios including overlapping of signals, encrypted information, and lack of accuracy in derived information are still challenging^[227]. Knowingly, the rapid reduction in output voltage occurred due to the removal of concurrent stimulus; thereby, Seebeck effect facilitated TE voltages in the presence of temperature differences^[228]. Likely, invisible thermal radiation induces temperature variations and realizes output voltage in a TE compound; thus, TE temperature sensors convert temperature stimuli into voltage signals for temperature detection^[229]. For instance, reliable voltage signals for low-temperature difference due to thermal radiation in a CNT/PEDOT:PSS/NFC (CPN) sensor lead to isothermal distribution; however, the presence of interlayer is beneficial to air hindrance and thus establishes temperature differences [Figure 12B]^[230]. Similarly, the CPN sensor exhibited impressive stimulus response to the variant temperatures resulting from their low thermal conductivity; e.g., Figure 12C shows the activation of the sensor upon touching the robotic finger with a hot plate at temperature $> 80\text{ }^{\circ}\text{C}$ and $< -40\text{ }^{\circ}\text{C}$ and corresponding prominent variations of 0.34 s and 0.45 s, respectively. Thus, the CPN sensor could be utilized in high-cold temperature environments to avoid any damage to electronics and extend the service life of the device. With this concept, the finger as an essential organ of the human body emerges in the next generation of human-machine interactions; i.e., the finger, being a stable thermal radiation emitter, can track and recognize the trajectories in the extended application of 4×4 noncontact sensor array due to their variation in TE voltage [Figure 12D]. This study establishes a route to other sensors based on the TE principle and elucidates that voltage difference may be sustained for extra time in future moderate sensors without any interference for integrated e-skins in the contact model.

Flexible thermoelectrics in human-machine interactions

Telluride-based glasses (Cu-Ge-Te, Cu-As-Se-Te, Ag-Ga₂Te₃-SnTe, and Ge-Se-Te) inspire high thermal-sensing performance; however, the available efforts of ChGs reveal unsuitable bulk form for wearable

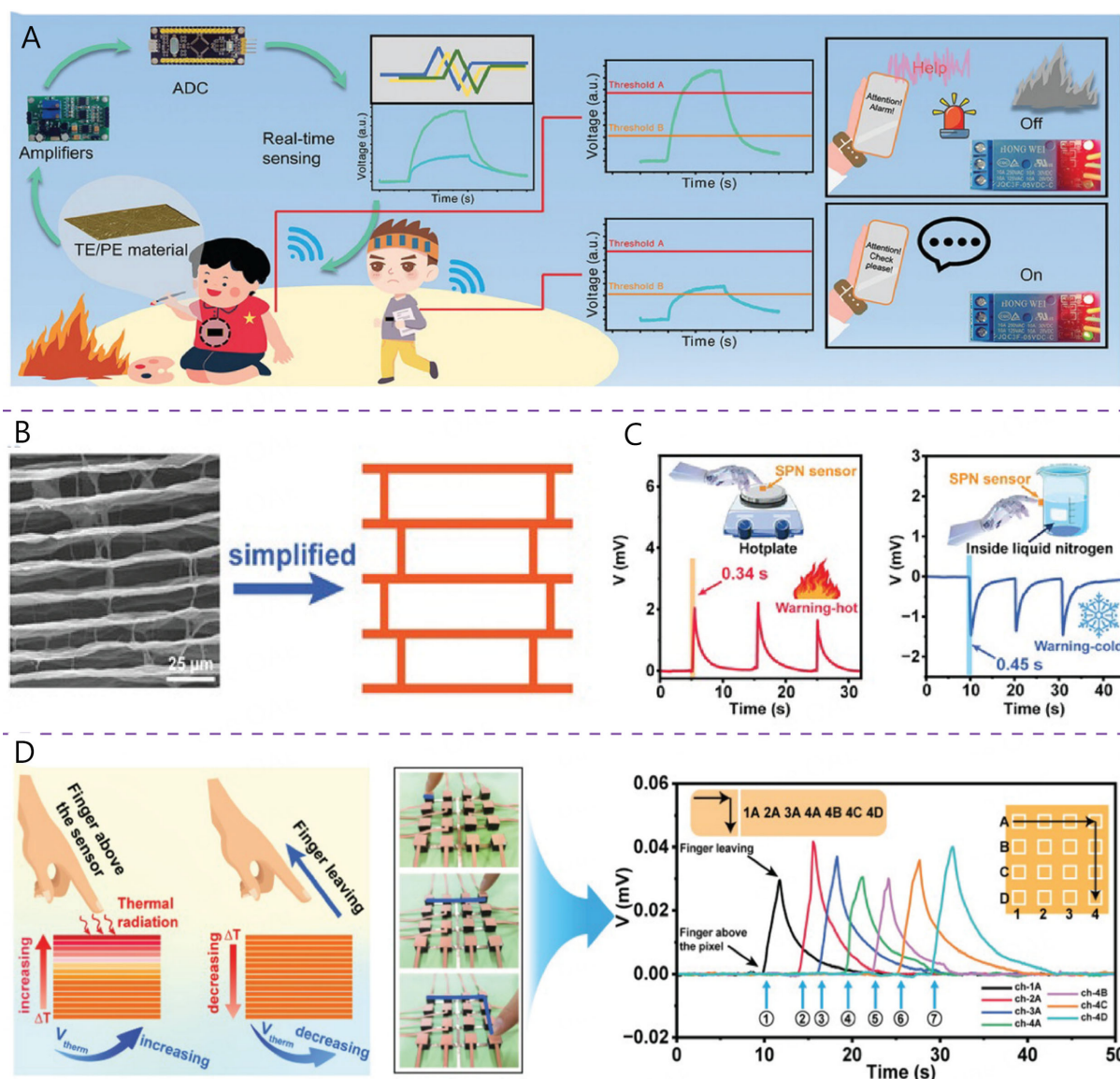


Figure 12. (A) TE and photoelectric dual modulated sensors for accurate fire recognition and warning for child fire protection^[226], Copyright 2023 Wiley-VCH GmbH (B) CPN sensor based on SEM image, (C) output voltage of CPN sensor under $>80\text{ }^{\circ}\text{C}$ and $<-40\text{ }^{\circ}\text{C}$, (D) illustration of the finger as a thermal radiation emitter and their corresponding movements^[230]. Copyright 2023 Wiley-VCH GmbH. CPN: CNT/PEDOT:PSS/NFC; TE: Flexible thermoelectric.

devices due to their uncontrolled crystallization during fiber drawing^[37,123]. Also, conventional fabrication of ChG films by magnetron sputtering, chemical vapor deposition and thermal evaporation demonstrated moderate flexibility without stretchability leading to restricted wearable applications^[231]. Therefore, a roll-to-roll strategy of polytetrafluoroethylene (PTFE) binders and ChG particles was proposed for flexible $\text{Cu}_{25}\text{As}_{35}\text{Se}_6\text{Te}_{34}$ -PTFE films^[223,232], and hence ultra flexible ChG film resulted in a sufficient Seebeck coefficient of $\sim 731\text{ }\mu\text{V/K}$ with high strain-sensing. In this aspect, the responses to relative resistance variations of 0.3 and 0.2 were observed with facial expressions frowning and smiling readily detected by CAST-PTFE films. Similarly, the adhered CAST-PTFE film to the throat and arm can easily monitor swallowing arm bending after each deformed action [Figure 13A], where the attached film with wrists and 3 mm-thick foam rubber continuously monitors the skin temperature. Moreover, variation of temperature difference at two sides of

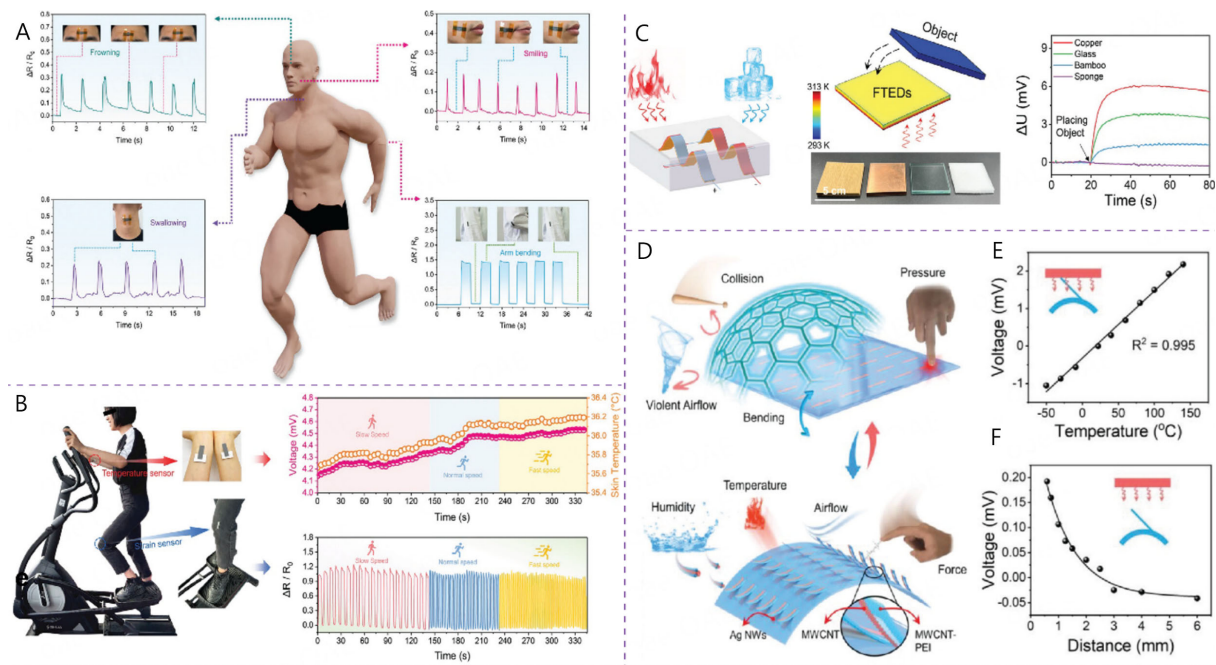


Figure 13. (A) Real-time monitoring of human motion with relative resistance variation of CAST-PTFE film at different human motions, and (B) real-time temperature and knee bending monitoring during human motion monitoring output voltage and relative resistance of CAST-PTFE film [232], Copyright 2024 Wiley-VCH GmbH (C) sensing object temperature and thermal conductivity of FTEDs and ΔU -time curve for different objects [235], Copyright 2024 Wiley-VCH GmbH (D) various sensing modalities for 2D and 3D structures, and (E, F) voltage-temperature curves for the sensor in 3D mode and heat proximity test at 40 °C [236]. Copyright 2024 Wiley-VCH GmbH. FTEDs: Flexible thermoelectric device; PTFE: polytetrafluoroethylene.

the film results in voltage output, and thus the status of speed can be monitored on the treadmill [Figure 13B]. Similarly, strain sensing of the film experiences a periodic change at the knee joint with repeatedly bending and relaxing; thus, a relative resistance by the film determined the speed of motion correspondingly.

It is known that skin exhibits an important sensory interface between the external environment and the human body [233]. In this scenario, e-skins may imitate mechanical and sensation features of natural skin, and thus realize extensively in next-generation wearable electronics. So far, efforts revealed that e-skins respond to pressure, flexion, and strain stimuli due to their deformation, and thus perceptual signals indicating other stimulus information [234]. For example, an electronic whisker characterized a typical 3D structure sensor demonstrated sensing modalities with detected out-of-plane stimuli including airflow and collision [62]. The incorporation of e-skin and e-whisker units into a device leads to stimulus signals comprehensively, while an all-in-one device makes the circuit design complicated and challenging. Therefore, a stretchable biomimetic multimodal receptor (SBMR) inspired by morphological switching of hummingbird feathers should facilitate the transformation of its 2D to 3D structure for MWCNT-based TE materials [Figure 13C, D] [235,236]. For instance, SBMR experiences the sense in a 2D flat mode such as pressure and bending, and thus deformation only results in negligible sensing as compared to 3D structure upon wind and collision. Moreover, a 3D pattern with TE layered SBMR operated for heat sensing by detecting ambient heat and humidity as sensory receptors due to change of voltage signals, however a maintained sensing performance during cyclic variation at receptor sense the heat proximity through temperature gradient across TE leg [Figure 13E, F]. The SBMR revealed impressive monitoring of various signals related to room humidity, and

air outlet airflow, thus opening the development of reliable and multifunction sensors in robotics.

Usually, TE legs in many flexible devices are thick and not conducive to the impressive ability of temperature sensing; thus, an integrating approach has always been needed for flexible interconnection with reasonable thickness between multiple rigid TEGs. In this aspect, a novel island-bridge interconnection approach was adopted to integrate the performance of inorganic micro-TEGs relative to their thickness for temperature sensing e-skin applications TEG (p-type $\text{Bi}_{0.5}\text{Sb}_{1.5}\text{Te}_3$, n-type Bi_2Te_3), as shown in Figure 14A^[42]. However, Ni and Au deposition improved the wettability and bonding strength of electrodes in TEG (p-type $\text{Bi}_{0.5}\text{Sb}_{1.5}\text{Te}_3$, n-type Bi_2Te_3). In the integration of TEG, PI-copper film and PDMS were considered for island-bridge structure in stretchable self-powered temperature electronic skin (STES), and hence as-prepared e-skin lead high sensitivity about $\sim 729 \mu\text{V K}^{-1}$ with ultrafast response of 0.157 s. Correspondingly, the sensor demonstrated low stretching cross-talk and good mechanical stability at temperature difference of 12 K with high consistency, indicating similar voltage response at different sensing units of STES [Figure 14B]. The sensing applications are illustrated in Figure 14C, where stretchable temperature sensor array as e-skin is attached to robot finger and senses the human finger at $\sim 32^\circ\text{C}$, cold water at $\sim 8^\circ\text{C}$, and hot water at $\sim 52^\circ\text{C}$ upon human-machine interaction. These STES open new perspectives for the noncontact spatial temperature-responsing, robotic thermosensing, etc.

CONCLUSIONS AND PROSPECTS

This review presents the research status of high-performance flexible TEs, their practical applications, and some effective approaches for improving power output in recent decades. Thus, the emerging strategies are detailed covering the mechanisms of charge transport in flexible TEs for power generation in textiles, wearable electronics, organic/inorganic sensors, etc. Flexible TE sensors in the wide-range applications of energy harvesting reveal the conversion of temperature gradient into voltage in many wearable electronics for human safety, robotics, health monitoring, etc. Ultimately, the recently developed effective methods predict the pathways for new materials and power generation capabilities in flexible TE systems; however, some technologies and their bottom-up approaches, along with the current challenges, are detailed in the sections below:

A comfortable attachment of solid-state devices with human skin for wearable devices in utilization is challenging. For better performance, such attachment in flexible TEs could be attained from good mechanical flexibility and wearability. Herein, future research has to be focused on micro-nano TE fibers utilizing a thermal drawing approach. Further, comprehensive research on cotton fabric may lead to the impressive flexibility and wearability utilizing fabrics-based materials.

Though some solid-state devices, including organic TEs (PEDOT:PSS, PEDOT: $\text{Fe}^{3+}(\text{O-tosylate})_3$, (PEDOT:Tos), polyetherimide (PEI)/SWCNT, etc.), led to impressive features; however, the major complexities of surface still limit their applications in flexible electronics. Herein, this review proposes more exploration of stretchable substrates through sputtering and inkjet printing. Thus, the new morphologies could optimize the charge transport in corresponding devices for health monitoring applications. Additionally, microstructure engineering could optimize thermal conductivity and Seebeck coefficients in conducting polymers and inorganic crystalline semiconductors. Consequently, the challenging temperature sensitivity could be managed through moderate strategies for optimizing the thermal conductivity and Seebeck coefficients of semiconducting ChGs.

So far, the organic TEs, including PPy and PEDOT, have resulted in great flexibility and sensitivity, while the major challenges in designing self-powered temperature devices still limit their applications owing to

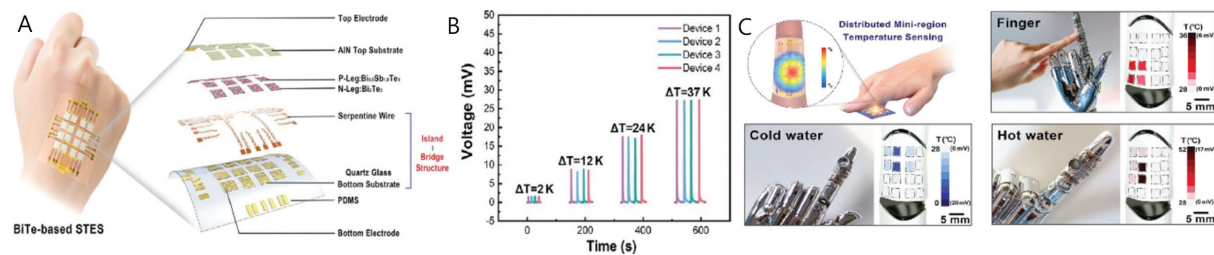


Figure 14. (A) Schematic of the STES representing their internal composition and structure, (B) sensing function of the STES, and (C) STES in self-powered distributed mini-region sensing with digital photos of a robotic hand wearing STES^[42]. Copyright 2023 Wiley-VCH GmbH.

modulus mismatch and lead to low stability and sensing accuracy. This review recommends future research on inorganic TEs with optimized Seebeck coefficients utilized in wearable devices for output voltage in health monitoring wearable technology. Additionally, the leakage and encapsulation of devices could further be explored with excellent mechanical features.

To understand and resolve the major challenges and core estimations of flexible thermoelectricity, image recognition algorithms and database-based extrapolation could be databased according to the available literature. As the investigation of flexible thermoelectricity by machine learning with moderate applications is very limited, some trained models and deep learning algorithms could be explored and thus a roadmap for ideal flexible TE materials with available experimental research, theoretical analysis, and numerical calculation at low cost could be realized. There is still a long and arduous way to the preparation and assembly of devices, while machine learning may provide a huge interest in flexible TE technology for humanity and industry. Thus, current waste heat needs to be managed by utilizing flexible TEDs industrially.

DECLARATIONS

Authors' contributions

Developed the concept: Basit, A.; Dai, JY.

Conducted the frame of the paper: Xin, J.; Li, X.

Collected the various works of literature: Hussain, T.; Wang, G.

Wrote the manuscript, helped to polish this paper: Basit, A.; Zheng, G.

All authors discussed the results.

Availability of data and materials

Not applicable.

Financial support and sponsorship

This work was supported by the Research Grants Council of Hong Kong Special Administrative Region, China (grant number: 15233823), and Guangdong–Hong Kong–Macao Joint Laboratory for Photonic-Thermal-Electrical Energy Materials and Devices (GDSTC No. 2019B121205001). Abdul Basit thanks the PolyU Postdoc Matching Fund support (B-QC6B).

Conflicts of interest

There are no conflicts of interest to declare.

Ethical approval and consent to participate

Not applicable.

Consent for publication

Not applicable.

REFERENCES

- Thakur, A. K.; Majumder, M.; Singh, S. B. Graphene and its derivatives for secondary battery application. In: Sahoo S, Tiwari SK, Nayak GC, editors. *Surface Engineering of Graphene*. Cham: Springer International Publishing; 2019. pp. 53-80. DOI
- Ahmad, H.; Kamarudin, S. K.; Minggu, L. J.; Hasran, U. A.; Masdar, S.; Wan, D. W. R. Enhancing methanol oxidation with a TiO₂ - modified semiconductor as a photo-catalyst. *Int. J. Hydrogen. Energy*. **2017**, *42*, 8986-96. DOI
- Selvan, K. V.; Hasan, M. N.; Mohamed, A. M. S. State-of-the-art reviews and analyses of emerging research findings and achievements of thermoelectric materials over the past years. *J. Electron. Mater.* **2019**, *48*, 745-77. DOI
- Novak, T. G.; Kim, J.; Kim, J.; et al. Complementary n-type and p-type graphene films for high power factor thermoelectric generators. *Adv. Funct. Materials*. **2020**, *30*, 2001760. DOI
- Stamenkovic, V. R.; Strmcnik, D.; Lopes, P. P.; Markovic, N. M. Energy and fuels from electrochemical interfaces. *Nat. Mater.* **2016**, *16*, 57-69. DOI PubMed
- Uher, C. Materials aspect of thermoelectricity. 2016. DOI
- Ravich, I. I. Semiconducting lead chalcogenides. 2013. 5. DOI
- Liu, W.; Tan, X.; Yin, K.; et al. Convergence of conduction bands as a means of enhancing thermoelectric performance of n-type Mg₂Si_{1-x}Sn_x solid solutions. *Phys. Rev. Lett.* **2012**, *108*, 166601. DOI
- Qian, X.; Wu, H.; Wang, D.; et al. Synergistically optimizing interdependent thermoelectric parameters of n-type PbSe through alloying CdSe. *Energy. Environ. Sci.* **2019**, *12*, 1969-78. DOI
- Jang, H.; Kim, S.; Park, I.; et al. Long-range ordered graphitic structure in silk fibers delaminated using dopamine and thermal treatment for super-flexible electronic textiles: Possible applications for magnetic and thermoelectric textiles. *Adv. Compos. Hybrid. Mater.* **2024**, *7*, 857. DOI
- Hsu, K. F.; Loo, S.; Guo, F.; et al. Cubic AgPb(m)SbTe(2+m): bulk thermoelectric materials with high figure of merit. *Science* **2004**, *303*, 818-21. DOI PubMed
- Li, J.; Zhang, X.; Lin, S.; Chen, Z.; Pei, Y. Realizing the high thermoelectric performance of GeTe by Sb-doping and Se-alloying. *Chem. Mater.* **2017**, *29*, 605-11. DOI
- Xiao, Y.; Zhao, L. Charge and phonon transport in PbTe-based thermoelectric materials. *npj. Quant. Mater.* **2018**, *3*, 127. DOI
- Hodges, J. M.; Hao, S.; Grovogui, J. A.; et al. Chemical insights into PbSe- x%HgSe: high power factor and improved thermoelectric performance by alloying with discordant atoms. *J. Am. Chem. Soc.* **2018**, *140*, 18115-23. DOI PubMed
- Tan, G.; Shi, F.; Hao, S.; et al. Codoping in SnTe: Enhancement of thermoelectric performance through synergy of resonance levels and band convergence. *J. Am. Chem. Soc.* **2015**, *137*, 5100-12. DOI
- Li, J.; Tan, Q.; Li, J.; et al. BiSbTe-based nanocomposites with High ZT : the effect of sic nanodispersion on thermoelectric properties. *Adv. Funct. Materials*. **2013**, *23*, 4317-23. DOI
- Fang, T.; Li, X.; Hu, C.; et al. Complex band structures and lattice dynamics of Bi₂Te₃-based compounds and solid solutions. *Adv. Funct. Materials*. **2019**, *29*, 1900677. DOI
- Mizuguchi, Y.; Nishida, A.; Omachi, A.; Miura, O.; Saini, N. L. Thermoelectric properties of new Bi-chalcogenide layered compounds. *Cogent. Physics*. **2016**, *3*. DOI
- Zhao, L. D.; Wu, H. J.; Hao, S. Q.; et al. All-scale hierarchical thermoelectrics: MgTe in PbTe facilitates valence band convergence and suppresses bipolar thermal transport for high performance. *Energy. Environ. Sci.* **2013**, *6*, 3346. DOI
- Rowe, D. Introduction. In: Rowe D, editor. *CRC Handbook of Thermoelectrics*. CRC Press; 1995. DOI
- Zhang, X.; Bu, Z.; Lin, S.; Chen, Z.; Li, W.; Pei, Y. GeTe Thermoelectrics. *Joule* **2020**, *4*, 986-1003. DOI
- Li, J.; Chen, Z.; Zhang, X.; Sun, Y.; Yang, J.; Pei, Y. Electronic origin of the high thermoelectric performance of GeTe among the p-type group IV monotellurides. *NPG. Asia. Mater.* **2017**, *9*, e353-e353. DOI
- Perumal, S.; Roychowdhury, S.; Negi, D. S.; Datta, R.; Biswas, K. High Thermoelectric performance and enhanced mechanical stability of p-type Ge_{1-x}Sb_xTe. *Chem. Mater.* **2015**, *27*, 7171-8. DOI
- Li, J.; Chen, Z.; Zhang, X.; et al. Simultaneous optimization of carrier concentration and alloy scattering for ultrahigh performance GeTe thermoelectrics. *Adv. Sci. (Weinh)*. **2017**, *4*, 1700341. DOI PubMed PMC
- Chen, Z.; Ge, B.; Li, W.; et al. Vacancy-induced dislocations within grains for high-performance PbSe thermoelectrics. *Nat. Commun.* **2017**, *8*, 13828. DOI PubMed PMC
- Liu, C.; Zhang, Z.; Peng, Y.; et al. Charge transfer engineering to achieve extraordinary power generation in GeTe-based thermoelectric materials. *Sci. Adv.* **2023**, *9*, eadh0713. DOI PubMed PMC
- Berman, R.; Klemens, P. G. Thermal conduction in solids. *Physics. Today*. **1978**, *31*, 56-7. DOI
- Donadio, D.; Galli, G. Atomistic simulations of heat transport in silicon nanowires. *Phys. Rev. Lett.* **2009**, *102*, 195901. DOI

PubMed

29. Biswas, K.; He, J.; Blum, I. D.; et al. High-performance bulk thermoelectrics with all-scale hierarchical architectures. *Nature* **2012**, *489*, 414-8. [DOI](#)
30. Snyder, G. J.; Toberer, E. S. Complex thermoelectric materials. *Nat. Mater.* **2008**, *7*, 105-14. [DOI](#) [PubMed](#)
31. Liang, L.; Lv, H.; Shi, X. L.; et al. A flexible quasi-solid-state thermoelectrochemical cell with high stretchability as an energy-autonomous strain sensor. *Mater. Horiz.* **2021**, *8*, 2750-60. [DOI](#)
32. Zhang, L.; Shi, X.; Yang, Y.; Chen, Z. Flexible thermoelectric materials and devices: From materials to applications. *Mater. Today.* **2021**, *46*, 62-108. [DOI](#)
33. Huang, L.; Lin, S.; Xu, Z.; et al. Fiber-based energy conversion devices for human-body energy harvesting. *Adv. Mater.* **2020**, *32*, e1902034. [DOI](#) [PubMed](#)
34. Yang, Q.; Yang, S.; Qiu, P.; et al. Flexible thermoelectrics based on ductile semiconductors. *Science* **2022**, *377*, 854-8. [DOI](#)
35. Shi, X.; Chen, H.; Hao, F.; et al. Room-temperature ductile inorganic semiconductor. *Nat. Mater.* **2018**, *17*, 421-6. [DOI](#)
36. Yang, S.; Gao, Z.; Qiu, P.; et al. Ductile Ag₂₀S₇Te₃ with excellent shape-conformability and high thermoelectric performance. *Adv. Mater.* **2021**, *33*, e2007681. [DOI](#)
37. Zhang, H.; Zhang, Y.; Chen, C.; Yu, P.; Wang, L. M.; Li, G. High-conductivity chalcogenide glasses in Ag-Ga₂Te₃-SnTe systems and their suitability as thermoelectric materials. *ACS. Appl. Mater. Interfaces.* **2023**, *15*, 19170-7. [DOI](#) [PubMed](#)
38. Gao, Z.; Yang, Q.; Qiu, P.; et al. p-Type plastic inorganic thermoelectric materials. *Adv. Energy. Mater.* **2021**, *11*, 2100883. [DOI](#)
39. Wang, Y.; Qiu, P.; Yang, S.; Gao, Z.; Chen, L.; Shi, X. Mechanical and thermoelectric properties in Te-rich Ag₂(Te,S) meta-phases. *J. Materiomics.* **2024**, *10*, 543-51. [DOI](#)
40. Yang, Q.; Ming, C.; Qiu, P.; et al. Incommensurately modulated structure in AgCuSe-based thermoelectric materials for intriguing electrical, thermal, and mechanical properties. *Small* **2023**, *19*, e2300699. [DOI](#)
41. Liang, J.; Wang, T.; Qiu, P.; et al. Flexible thermoelectrics: from silver chalcogenides to full-inorganic devices. *Energy. Environ. Sci.* **2019**, *12*, 2983-90. [DOI](#)
42. Kang, M.; Qu, R.; Sun, X.; et al. Self-powered temperature electronic skin based on island-bridge structure and Bi-Te micro-thermoelectric generator for distributed mini-region sensing. *Adv. Mater.* **2023**, *35*, e2309629. [DOI](#) [PubMed](#)
43. Aguayo-Tapia, S.; Avalos-Almazan, G.; Rangel-Magdaleno, J. J. Entropy-based methods for motor fault detection: a review. *Entropy. (Basel).* **2024**, *26*, 299. [DOI](#) [PubMed](#) [PMC](#)
44. Yuan, J.; Zhang, Y.; Wei, C.; Zhu, R. A fully self-powered wearable leg movement sensing system for human health monitoring. *Adv. Sci. (Weinh).* **2023**, *10*, e2303114. [DOI](#) [PubMed](#) [PMC](#)
45. Hou, Y.; Yang, Y.; Wang, Z.; et al. Whole fabric-assisted thermoelectric devices for wearable electronics. *Adv. Sci. (Weinh).* **2022**, *9*, e2103574. [DOI](#) [PubMed](#) [PMC](#)
46. Lee, B.; Cho, H.; Park, K. T.; et al. High-performance compliant thermoelectric generators with magnetically self-assembled soft heat conductors for self-powered wearable electronics. *Nat. Commun.* **2020**, *11*, 5948. [DOI](#) [PubMed](#) [PMC](#)
47. Liu, Y.; Hou, S.; Wang, X.; et al. Passive radiative cooling enables improved performance in wearable thermoelectric generators. *Small* **2022**, *18*, e2106875. [DOI](#)
48. Twaha, S.; Zhu, J.; Yan, Y.; Li, B. A comprehensive review of thermoelectric technology: Materials, applications, modelling and performance improvement. *Renew. Sustain. Energy. Rev.* **2016**, *65*, 698-726. [DOI](#)
49. Nozariasbmarz, A.; Collins, H.; Dsouza, K.; et al. Review of wearable thermoelectric energy harvesting: From body temperature to electronic systems. *Appl. Energy.* **2020**, *258*, 114069. [DOI](#)
50. Jiang, Y.; Dong, J.; Zhuang, H. L.; et al. Evolution of defect structures leading to high ZT in GeTe-based thermoelectric materials. *Nat. Commun.* **2022**, *13*, 6087. [DOI](#) [PubMed](#) [PMC](#)
51. Spann, B. T.; Weber, J. C.; Brubaker, M. D.; et al. Semiconductor thermal and electrical properties decoupled by localized phonon resonances. *Adv. Mater.* **2023**, *35*, e2209779. [DOI](#) [PubMed](#)
52. Tarascon, J.; Armand, M. Issues and challenges facing rechargeable lithium batteries. Materials for Sustainable Energy. Co-Published with Macmillan Publishers Ltd, UK; 2010. pp. 171-9. [DOI](#)
53. Yin, L.; Kim, K. N.; Trifonov, A.; Podhajny, T.; Wang, J. Designing wearable microgrids: towards autonomous sustainable on-body energy management. *Energy. Environ. Sci.* **2022**, *15*, 82-101. [DOI](#)
54. Yan, Q.; Kanatzidis, M. G. High-performance thermoelectrics and challenges for practical devices. *Nat. Mater.* **2022**, *21*, 503-13. [DOI](#) [PubMed](#)
55. Kim, F.; Kwon, B.; Eom, Y.; et al. 3D printing of shape-conformable thermoelectric materials using all-inorganic Bi₂Te₃-based inks. *Nat. Energy.* **2018**, *3*, 301-9. [DOI](#)
56. Chowdhury, I.; Prasher, R.; Lofgreen, K.; et al. On-chip cooling by superlattice-based thin-film thermoelectrics. *Nat. Nanotechnol.* **2009**, *4*, 235-8. [DOI](#)
57. Li, G.; Garcia, F. J.; Lara, R. D. A.; et al. Integrated microthermoelectric coolers with rapid response time and high device reliability. *Nat. Electron.* **2018**, *1*, 555-61. [DOI](#)
58. Snyder, G. J.; Lim, J. R.; Huang, C. K.; Fleurial, J. P. Thermoelectric microdevice fabricated by a MEMS-like electrochemical process. *Nat. Mater.* **2003**, *2*, 528-31. [DOI](#) [PubMed](#)
59. Morelli, D. T.; Meisner, G. P. Low temperature properties of the filled skutterudite CeFe₄Sb₁₂. *Journal. of. Applied. Physics.* **1995**, *77*, 3777-81. [DOI](#)

60. Yan, X.; Poudel, B.; Ma, Y.; et al. Experimental studies on anisotropic thermoelectric properties and structures of n-type $\text{Bi}_2\text{Te}_{2.7}\text{Se}_{0.3}$. *Nano. Lett.* **2010**, *10*, 3373–8. DOI PubMed
61. Yang, J. C.; Mun, J.; Kwon, S. Y.; Park, S.; Bao, Z.; Park, S. Electronic skin: recent progress and future prospects for skin-attachable devices for health monitoring, robotics, and prosthetics. *Adv. Mater.* **2019**, *31*, e1904765. DOI PubMed
62. Chun, S.; Kim, J.; Yoo, Y.; et al. An artificial neural tactile sensing system. *Nat. Electron.* **2021**, *4*, 429–38. DOI
63. Pyo, S.; Lee, J.; Bae, K.; Sim, S.; Kim, J. Recent progress in flexible tactile sensors for human-interactive systems: from sensors to advanced applications. *Adv. Mater.* **2021**, *33*, e2005902. DOI PubMed
64. Wei, Y.; Li, X.; Wang, Y.; et al. Graphene-based multifunctional textile for sensing and actuating. *ACS. Nano.* **2021**, *15*, 17738–47. DOI
65. Jung, Y. H.; Hong, S. K.; Wang, H. S.; et al. Flexible piezoelectric acoustic sensors and machine learning for speech processing. *Adv. Mater.* **2020**, *32*, e1904020. DOI PubMed
66. Fan, F.; Tian, Z.; Lin, W. Z. Flexible triboelectric generator. *Nano. Energy.* **2012**, *1*, 328–34. DOI
67. Zhou, Q.; Ji, B.; Hu, F.; et al. Magnetized microcilia array-based self-powered electronic skin for micro-scaled 3D morphology recognition and high-capacity communication. *Adv. Funct. Materials.* **2022**, *32*, 2208120. DOI
68. Cao, Z.; Yang, Y.; Zheng, Y.; et al. Highly flexible and sensitive temperature sensors based on $\text{Ti}_3\text{C}_2\text{T}_x$ (MXene) for electronic skin. *J. Mater. Chem. A.* **2019**, *7*, 25314–23. DOI
69. Bermúdez GS, Makarov D. Magnetosensitive e-skins for interactive devices. *Adv. Funct. Materials.* **2021**, *31*, 2007788. DOI
70. Lu, L.; Jiang, C.; Hu, G.; Liu, J.; Yang, B. Flexible noncontact sensing for human-machine interaction. *Adv. Mater.* **2021**, *33*, e2100218. DOI
71. Sun, T.; Zhou, B.; Zheng, Q.; Wang, L.; Jiang, W.; Snyder, G. J. Stretchable fabric generates electric power from woven thermoelectric fibers. *Nat. Commun.* **2020**, *11*, 572. DOI PubMed PMC
72. Wang, Y.; Liu, K.; Zhao, W.; et al. Antibacterial fabrics based on synergy of piezoelectric effect and physical interaction. *Nano. Today.* **2023**, *48*, 101737. DOI
73. Qiu, W.; Feng, Y.; Luo, N.; Chen, S.; Wang, D. Sandwich-like sound-driven triboelectric nanogenerator for energy harvesting and electrochromic based on Cu foam. *Nano. Energy.* **2020**, *70*, 104543. DOI
74. Chen, Z.; Guan, X.; Wen, N.; Pan, L.; Fan, Z. Construction of flexible, self-supporting, and in-plane anisotropic PEDOT:PSS thermoelectric films via the wet-winding approach. *ACS. Appl. Polym. Mater.* **2023**, *5*, 2905–16. DOI
75. Li, Y. Y.; Qin, X. Y.; Li, D.; et al. Enhanced thermoelectric performance of $\text{Cu}_2\text{Se}/\text{Bi}_{0.4}\text{Sb}_{1.6}\text{Te}_3$ nanocomposites at elevated temperatures. *Appl. Phys. Lett.* **2016**, *108*, 062104. DOI
76. Cao, T.; Shi, X.; Chen, Z. Advances in the design and assembly of flexible thermoelectric device. *Prog. Mater. Sci.* **2023**, *131*, 101003. DOI
77. Lee, T.; Park, K. T.; Ku, B. C.; Kim, H. Carbon nanotube fibers with enhanced longitudinal carrier mobility for high-performance all-carbon thermoelectric generators. *Nanoscale* **2019**, *11*, 16919–27. DOI PubMed
78. Zhang, T.; Li, K.; Zhang, J.; et al. High-performance, flexible, and ultralong crystalline thermoelectric fibers. *Nano. Energy.* **2017**, *41*, 35–42. DOI
79. Shalini, V.; Harish, S.; Archana, J.; Ikeda, H.; Navaneethan, M. Interface effect and band engineering in $\text{Bi}_2\text{Te}_3/\text{C}$ and $\text{Bi}_2\text{Te}_3/\text{Ni-Cu}$ with enhanced thermopower for self-powered wearable thermoelectric generator. *J. Alloys. Compd.* **2021**, *868*, 158905. DOI
80. Yang, Z. Y.; Jin, X. Z.; Huang, C. H.; Lei, Y. Z.; Wang, Y. Constructing A/B-Side heterogeneous asynchronous structure with Ag_2Se layers and bushy-like PPy toward high-performance flexible photo-thermoelectric generators. *ACS. Appl. Mater. Interfaces.* **2022**, *14*, 33370–82. DOI PubMed
81. Lu, Y.; Qiu, Y.; Cai, K.; et al. Ultrahigh performance PEDOT/ $\text{Ag}_2\text{Se}/\text{CuAgSe}$ composite film for wearable thermoelectric power generators. *Mater. Today. Phys.* **2020**, *14*, 100223. DOI
82. Hou, S.; Liu, Y.; Yin, L.; et al. High performance wearable thermoelectric generators using Ag_2Se films with large carrier mobility. *Nano. Energy.* **2021**, *87*, 106223. DOI
83. He, X.; Shi, J.; Hao, Y.; et al. Highly stretchable, durable, and breathable thermoelectric fabrics for human body energy harvesting and sensing. *Carbon. Energy.* **2022**, *4*, 621–32. DOI
84. Lucas, P.; Conseil, C.; Yang, Z.; et al. Thermoelectric bulk glasses based on the Cu–As–Te–Se system. *J. Mater. Chem. A.* **2013**, *1*, 8917. DOI
85. Jia, Y.; Jiang, Q.; Sun, H.; et al. Wearable thermoelectric materials and devices for self-powered electronic systems. *Adv. Mater.* **2021**, *33*, e2102990. DOI PubMed
86. Yuan, X.; Li, Z.; Shao, Y.; et al. Bi_2Te_3 -based wearable thermoelectric generator with high power density: from structure design to application. *J. Mater. Chem. C.* **2022**, *10*, 6456–63. DOI
87. Yao, H.; Fan, Z.; Cheng, H.; et al. Recent development of thermoelectric polymers and composites. *Macromol. Rapid. Commun.* **2018**, *39*, e1700727. DOI
88. Wang, H.; Yu, C. Organic Thermoelectrics: materials preparation, performance optimization, and device integration. *Joule* **2019**, *3*, 53–80. DOI
89. Li, M.; Hong, M.; Dargusch, M.; Zou, J.; Chen, Z. High-efficiency thermocells driven by thermo-electrochemical processes. *Trends. Chem.* **2021**, *3*, 561–74. DOI
90. Song, W.; Liu, X.; Li, T.; et al. The strategy of achieving flexibility in materials and configuration of flexible lithium-ion batteries.

- Energy. Tech.* **2021**, *9*, 2100539. DOI
91. Hong, X.; Mei, J.; Wen, L.; et al. Nonlithium metal-sulfur batteries: steps toward a leap. *Adv. Mater.* **2019**, *31*, e1802822. DOI PubMed
 92. Cui, Y.; He, X.; Liu, W.; Zhu, S.; Zhou, M.; Wang, Q. Highly stretchable, sensitive, and multifunctional thermoelectric fabric for synergistic-sensing systems of human signal monitoring. *Adv. Fiber. Mater.* **2024**, *6*, 170-80. DOI
 93. Luo, Y.; Zhao, L.; Luo, G.; et al. Highly sensitive piezoresistive and thermally responsive fibrous networks from the in situ growth of PEDOT on MWCNT-decorated electrospun PU fibers for pressure and temperature sensing. *Microsyst. Nanoeng.* **2023**, *9*, 113. DOI PubMed PMC
 94. Li, T. T.; Fan, X. X.; Zhang, X.; Zhang, X.; Lou, C. W.; Lin, J. H. Photothermoelectric synergistic hydrovoltaic effect: a flexible photothermoelectric yarn panel for multiple renewable-energy harvesting. *ACS. Appl. Mater. Interfaces.* **2023**, DOI
 95. Ma, H.; Pu, S.; Wu, H.; et al. Flexible Ag₂Se thermoelectric films enable the multifunctional thermal perception in electronic skins. *ACS. Appl. Mater. Interfaces.* **2024**, *16*, 7453-62. DOI
 96. Hyland, M.; Hunter, H.; Liu, J.; Veety, E.; Vashae, D. Wearable thermoelectric generators for human body heat harvesting. *Appl. Energy.* **2016**, *182*, 518-24. DOI
 97. Chen, G.; Li, Y.; Bick, M.; Chen, J. Smart textiles for electricity generation. *Chem. Rev.* **2020**, *120*, 3668-720. DOI
 98. Elmoughni, H. M.; Atalay, O.; Ozlem, K.; Menon, A. K. Thermoelectric clothing for body heat harvesting and personal cooling: design and fabrication of a textile-integrated flexible and vertical device. *Energy. Tech.* **2022**, *10*, 2200528. DOI
 99. Zheng, Y.; Han, X.; Yang, J.; et al. Durable, stretchable and washable inorganic-based woven thermoelectric textiles for power generation and solid-state cooling. *Energy. Environ. Sci.* **2022**, *15*, 2374-85. DOI
 100. Kwon, C.; Lee, S.; Won, C.; et al. Multi-functional and stretchable thermoelectric Bi₂Te₃ fabric for strain, pressure, and temperature-sensing. *Adv. Funct. Materials.* **2023**, *33*, 2300092. DOI
 101. Hajji, M.; Absike, H.; Labrim, H.; Ez-zahraoui, H.; Benaissa, M.; Benyoussef, A. Strain effects on the electronic and thermoelectric properties of Bi₂Te₃: A first principles study. *Comput. Condens. Matter.* **2018**, *16*, e00299. DOI
 102. Li, N.; Wang, Q.; Shen, C.; et al. Large-scale flexible and transparent electronics based on monolayer molybdenum disulfide field-effect transistors. *Nat. Electron.* **2020**, *3*, 711-7. DOI
 103. Liu, S.; Zhang, M.; Kong, J.; Li, H.; He, C. Flexible, durable, green thermoelectric composite fabrics for textile-based wearable energy harvesting and self-powered sensing. *Compos. Sci. Technol.* **2023**, *243*, 110245. DOI
 104. Suarez, F.; Nozariasbmarz, A.; Vashae, D.; Öztürk, M. C. Designing thermoelectric generators for self-powered wearable electronics. *Energy. Environ. Sci.* **2016**, *9*, 2099-113. DOI
 105. Shen, D.; Xiao, M.; Zou, G.; Liu, L.; Duley, W. W.; Zhou, Y. N. Self-powered wearable electronics based on moisture enabled electricity generation. *Adv. Mater.* **2018**, *30*, e1705925. DOI PubMed
 106. Liu, L.; Wu, J.; Wu, L.; et al. Phase-selective synthesis of 1T' MoS₂ monolayers and heterophase bilayers. *Nat. Mater.* **2018**, *17*, 1108-14. DOI PubMed
 107. Xue, Y.; Cao, Y.; Luo, P.; et al. Asymmetric sandwich janus structure for high-performance textile-based thermo-hydroelectric generators toward human health monitoring. *Adv. Funct. Materials.* **2024**, *34*, 2310485. DOI
 108. Wen, N.; Guan, X.; Zuo, X.; et al. Investigations of morphology and carrier transport characteristics in high-performance PEDOT:PSS/tellurium binary composite fibers produced via continuous wet-spinning. *Adv. Funct. Materials.* **2024**, *34*, 2315677. DOI
 109. Wang, X.; Liang, L.; Lv, H.; Zhang, Y.; Chen, G. Elastic aerogel thermoelectric generator with vertical temperature-difference architecture and compression-induced power enhancement. *Nano. Energy.* **2021**, *90*, 106577. DOI
 110. Zhang, L.; Lin, S.; Hua, T.; Huang, B.; Liu, S.; Tao, X. Fiber-based thermoelectric generators: materials, device structures, fabrication, characterization, and applications. *Adv. Energy. Mater.* **2018**, *8*, 1700524. DOI
 111. Kim, D. H.; Lu, N.; Ma, R.; et al. Epidermal electronics. *Science* **2011**, *333*, 838-43. DOI
 112. Jeong, J. W.; McCall, J. G.; Shin, G.; et al. Wireless optofluidic systems for programmable in vivo pharmacology and optogenetics. *Cell* **2015**, *162*, 662-74. DOI PubMed PMC
 113. Kim, E. S.; Hwang, J. Y.; Lee, K. H.; Ohta, H.; Lee, Y. H.; Kim, S. W. Graphene substrate for van der waals epitaxy of layer-structured bismuth antimony telluride thermoelectric film. *Adv. Mater.* **2017**, *29*. DOI PubMed
 114. Jin, Q.; Zhao, Y.; Long, X.; et al. Flexible carbon nanotube-epitaxially grown nanocrystals for micro-thermoelectric modules. *Adv. Mater.* **2023**, *35*, e2304751. DOI PubMed
 115. Xu, N.; Zhu, P.; Sheng, Y.; et al. Synergistic tandem solar electricity-water generators. *Joule* **2020**, *4*, 347-58. DOI
 116. Zhu, P.; Shi, C.; Wang, Y.; et al. Recyclable, healable, and stretchable high-power thermoelectric generator. *Adv. Energy. Mater.* **2021**, *11*, 2100920. DOI
 117. Kraemer, D.; Poudel, B.; Feng, H. P.; et al. High-performance flat-panel solar thermoelectric generators with high thermal concentration. *Nat. Mater.* **2011**, *10*, 532-8. DOI
 118. Fukui, T.; Kawai, S.; Fujinuma, S.; et al. Control over differentiation of a metastable supramolecular assembly in one and two dimensions. *Nat. Chem.* **2017**, *9*, 493-9. DOI
 119. Zhuo, M.; Tao, Y.; Wang, X.; et al. 2D organic photonics: an asymmetric optical waveguide in self-assembled halogen-bonded cocrystals. *Angew. Chem.* **2018**, *130*, 11470-4. DOI
 120. Zhen, X.; Pu, K.; Jiang, X. Photoacoustic imaging and photothermal therapy of semiconducting polymer nanoparticles: signal

- amplification and second near-infrared construction. *Small* **2021**, *17*, e2004723. DOI PubMed
121. Xu, J.; Chen, Q.; Li, S.; et al. Charge-transfer cocrystal via a persistent radical cation acceptor for efficient solar-thermal conversion. *Angew. Chem.* **2022**, *134*, e202202571. DOI
 122. Kim, B.; Shin, H.; Park, T.; Lim, H.; Kim, E. NIR-sensitive poly(3,4-ethylenedioxyphenylene) derivatives for transparent photo-thermo-electric converters. *Adv. Mater.* **2013**, *25*, 5483-9. DOI PubMed
 123. Zhang, T.; Wang, Z.; Srinivasan, B.; et al. Ultraflexible glassy semiconductor fibers for thermal sensing and positioning. *ACS. Appl. Mater. Interfaces.* **2019**, *11*, 2441-7. DOI
 124. Lü, B.; Chen, Y.; Li, P.; Wang, B.; Müllen, K.; Yin, M. Stable radical anions generated from a porous perylenediimide metal-organic framework for boosting near-infrared photothermal conversion. *Nat. Commun.* **2019**, *10*, 767. DOI PubMed PMC
 125. Zhao, Y. D.; Han, J.; Chen, Y.; et al. Organic charge-transfer cocrystals toward large-area nanofiber membrane for photothermal conversion and imaging. *ACS. Nano.* **2022**, *16*, 15000-7. DOI
 126. Zhao, Y. D.; Jiang, W.; Zhuo, S.; et al. Stretchable photothermal membrane of NIR-II charge-transfer cocrystal for wearable solar thermoelectric power generation. *Sci. Adv.* **2023**, *9*, eadh8917. DOI PubMed PMC
 127. Yan, W.; Dong, C.; Xiang, Y.; et al. Thermally drawn advanced functional fibers: New frontier of flexible electronics. *Mater. Today.* **2020**, *35*, 168-94. DOI
 128. Loke, G.; Yan, W.; Khudiyev, T.; Noel, G.; Fink, Y. Recent progress and perspectives of thermally drawn multimaterial fiber electronics. *Adv. Mater.* **2020**, *32*, e1904911. DOI PubMed
 129. Zhang, J.; Zhang, T.; Zhang, H.; et al. Single-crystal SnSe thermoelectric fibers via laser-induced directional crystallization: from 1D fibers to multidimensional fabrics. *Adv. Mater.* **2020**, *32*, e2002702. DOI PubMed
 130. Sun, M.; Tang, G.; Huang, B.; et al. Tailoring microstructure and electrical transportation through tensile stress in Bi₂Te₃ thermoelectric fibers. *J. Materiomics.* **2020**, *6*, 467-75. DOI
 131. Sun, M.; Tang, G.; Wang, H.; et al. Enhanced Thermoelectric Properties of Bi₂Te₃-Based Micro-Nano Fibers via Thermal Drawing and Interfacial Engineering. *Adv. Mater.* **2022**, *34*, e2202942. DOI PubMed
 132. Zhang, X.; Shiu, B.; Li, T.; et al. Synergistic work of photo-thermoelectric and hydroelectric effects of hierarchical structure photo-thermoelectric textile for solar energy harvesting and solar steam generation simultaneously. *Chem. Eng. J.* **2021**, *426*, 131923. DOI
 133. Novoselov, K. S.; Geim, A. K.; Morozov, S. V.; et al. Electric field effect in atomically thin carbon films. *Science* **2004**, *306*, 666-9. DOI
 134. Zhang, Y.; Tan, Y. W.; Stormer, H. L.; Kim, P. Experimental observation of the quantum Hall effect and Berry's phase in graphene. *Nature* **2005**, *438*, 201-4. DOI PubMed
 135. Gupta, S.; Navaraj, W. T.; Lorenzelli, L.; Dahiya, R. Ultra-thin chips for high-performance flexible electronics. *npj. Flex. Electron.* **2018**, *2*, 21. DOI
 136. Niu, Q.; Peng, Q.; Lu, L.; et al. Single molecular layer of silk nanoribbon as potential basic building block of silk materials. *ACS. Nano.* **2018**, *12*, 11860-70. DOI
 137. Jeon, J. W.; Cho, S. Y.; Jeong, Y. J.; et al. Pyroprotein-based electronic textiles with high stability. *Adv. Mater.* **2017**, *29*. DOI PubMed
 138. Wang, C.; Li, X.; Gao, E.; et al. Carbonized silk fabric for ultrastretchable, highly sensitive, and wearable strain sensors. *Adv. Mater.* **2016**, *28*, 6640-8. DOI PubMed
 139. Lee, H.; Dellatore, S. M.; Miller, W. M.; Messersmith, P. B. Mussel-inspired surface chemistry for multifunctional coatings. *Science* **2007**, *318*, 426-30. DOI PubMed PMC
 140. He, G.; Xu, M.; Zhao, J.; et al. Bioinspired ultrastrong solid electrolytes with fast proton conduction along 2D channels. *Adv. Mater.* **2017**, *29*. DOI
 141. Liu, T.; Zhang, R.; Chen, M.; et al. Vertically aligned polyamidoxime/graphene oxide hybrid sheets' membrane for ultrafast and selective extraction of uranium from seawater. *Adv. Funct. Materials.* **2022**, *32*, 2111049. DOI
 142. Bubnova, O.; Khan, Z. U.; Malti, A.; et al. Optimization of the thermoelectric figure of merit in the conducting polymer poly(3,4-ethylenedioxythiophene). *Nat. Mater.* **2011**, *10*, 429-33. DOI PubMed
 143. Du, C.; Cao, M.; Li, G.; et al. Toward precision recognition of complex hand motions: wearable thermoelectrics by synergistic 2D nanostructure confinement and controlled reduction. *Adv. Funct. Materials.* **2022**, *32*, 2206083. DOI
 144. Chung, T.; Kaufman, J. H.; Heeger, A. J.; Wudl, F. Charge storage in doped poly(thiophene): Optical and electrochemical studies. *Phys. Rev. B.* **1984**, *30*, 702-10. DOI
 145. Li, Z.; Xu, Y.; Wu, L.; Cui, J.; Dou, H.; Zhang, X. Enabling giant thermopower by heterostructure engineering of hydrated vanadium pentoxide for zinc ion thermal charging cells. *Nat. Commun.* **2023**, *14*, 6816. DOI PubMed PMC
 146. Kwon, D. A.; Lee, S.; Kim, C. Y.; Kang, I.; Park, S.; Jeong, J. W. Body-temperature softening electronic ink for additive manufacturing of transformative bioelectronics via direct writing. *Sci. Adv.* **2024**, *10*, eadn1186. DOI PubMed PMC
 147. Byun, S.; Sim, J.; Agno, K.; Jeong, J. Materials and manufacturing strategies for mechanically transformative electronics. *Mater. Today. Adv.* **2020**, *7*, 100089. DOI
 148. Byun, S. H.; Kim, C. S.; Agno, K. C.; et al. Design strategy for transformative electronic system toward rapid, bidirectional stiffness tuning using graphene and flexible thermoelectric device interfaces. *Adv. Mater.* **2021**, *33*, e2007239. DOI PubMed
 149. Byun, S. H.; Yun, J. H.; Heo, S. Y.; et al. Self-cooling gallium-based transformative electronics with a radiative cooler for reliable stiffness tuning in outdoor use. *Adv. Sci. (Weinh).* **2022**, *9*, e2202549. DOI PubMed PMC

150. Lin, Y.; Genzer, J.; Dickey, M. D. Attributes, fabrication, and applications of gallium-based liquid metal particles. *Adv. Sci. (Weinh)*. **2020**, *7*, 2000192. DOI PubMed PMC
151. Lei, Z.; Gao, W.; Wu, P. Double-network thermocells with extraordinary toughness and boosted power density for continuous heat harvesting. *Joule* **2021**, *5*, 2211-22. DOI
152. Ding, T.; Zhou, Y.; Wang, X.; et al. All-soft and stretchable thermogalvanic gel fabric for antideformity body heat harvesting wearable. *Adv. Energy. Mater.* **2021**, *11*, 2102219. DOI
153. Xu, C.; Sun, Y.; Zhang, J.; Xu, W.; Tian, H. Adaptable and wearable thermocell based on stretchable hydrogel for body heat harvesting. *Adv. Energy. Mater.* **2022**, *12*, 2201542. DOI
154. Sun, M.; Qian, Q.; Tang, G.; et al. Enhanced thermoelectric properties of polycrystalline Bi₂Te₃ core fibers with preferentially oriented nanosheets. *APL Mater.* **2018**, *6*, 036103. DOI
155. Fu, Y.; Kang, S.; Gu, H.; et al. Superflexible inorganic Ag₂Te_{0.6}S_{0.4} fiber with high thermoelectric performance. *Adv. Sci. (Weinh)*. **2023**, *10*, e2207642. DOI PubMed PMC
156. Sun, Y.; Sheng, P.; Di, C.; et al. Organic thermoelectric materials and devices based on p- and n-type poly(metal 1,1,2,2-ethenetetrathiolate)s. *Adv. Mater.* **2012**, *24*, 932-7. DOI PubMed
157. Li, J.; Huckleby, A. B.; Zhang, M. Polymer-based thermoelectric materials: A review of power factor improving strategies. *J. Materiomics*. **2022**, *8*, 204-20. DOI
158. Lee, C.; Park, Y.; Hashimoto, H. Effect of nonstoichiometry on the thermoelectric properties of a Ag₂Se alloy prepared by a mechanical alloying process. *J. Appl. Phys.* **2007**, *101*, 024920. DOI
159. Kim, S. I.; Lee, K. H.; Mun, H. A.; et al. Thermoelectrics. Dense dislocation arrays embedded in grain boundaries for high-performance bulk thermoelectrics. *Science* **2015**, *348*, 109-14. DOI
160. Deng, T.; Gao, Z.; Qiu, P.; et al. High thermoelectric power factors in plastic/ductile bulk SnSe₂-based crystals. *Adv. Mater.* **2024**, *36*, e2304219. DOI PubMed
161. Liu, J.; Xing, T.; Gao, Z.; et al. Enhanced thermoelectric performance in ductile Ag₂S-based materials via doping iodine. *Appl. Phys. Lett.* **2021**, *119*, 121905. DOI
162. Liang, X.; Chen, C. Ductile inorganic amorphous/crystalline composite Ag₄TeS with phonon-glass electron-crystal transport behavior and excellent stability of high thermoelectric performance on plastic deformation. *Acta. Materialia*. **2021**, *218*, 117231. DOI
163. He, S.; Li, Y.; Liu, L.; et al. Semiconductor glass with superior flexibility and high room temperature thermoelectric performance. *Sci. Adv.* **2020**, *6*, eaaz8423. DOI PubMed PMC
164. Kim, G. H.; Shao, L.; Zhang, K.; Pipe, K. P. Engineered doping of organic semiconductors for enhanced thermoelectric efficiency. *Nat. Mater.* **2013**, *12*, 719-23. DOI
165. Lu, Y.; Ding, Y.; Qiu, Y.; et al. Good Performance and Flexible PEDOT:PSS/Cu₂Se Nanowire Thermoelectric Composite Films. *ACS Appl. Mater. Interfaces*. **2019**, *11*, 12819-29. DOI PubMed
166. Qu, S.; Yao, Q.; Wang, L.; et al. Highly anisotropic P3HT films with enhanced thermoelectric performance via organic small molecule epitaxy. *NPG. Asia. Mater.* **2016**, *8*, e292-e292. DOI
167. Liu, Y.; Aziguli, H.; Zhang, B.; et al. Ferroelectric polymers exhibiting behaviour reminiscent of a morphotropic phase boundary. *Nature* **2018**, *562*, 96-100. DOI
168. Li, F.; Lin, D.; Chen, Z.; et al. Ultrahigh piezoelectricity in ferroelectric ceramics by design. *Nat. Mater.* **2018**, *17*, 349-54. DOI
169. Liang, J.; Qiu, P.; Zhu, Y.; et al. Crystalline structure-dependent mechanical and thermoelectric performance in Ag₂Se_{1-x}S_x system. *Research. (Wash. D. C)*. **2020**, *2020*, 6591981. DOI PubMed PMC
170. Liang, J.; Liu, J.; Qiu, P.; et al. Modulation of the morphotropic phase boundary for high-performance ductile thermoelectric materials. *Nat. Commun.* **2023**, *14*, 8442. DOI PubMed PMC
171. Waqar, M.; Wu, H.; Chen, J.; Yao, K.; Wang, J. Evolution from lead-based to lead-free piezoelectrics: engineering of lattices, domains, boundaries, and defects leading to giant response. *Adv. Mater.* **2022**, *34*, e2106845. DOI PubMed
172. Li, C.; Jiang, F.; Liu, C.; et al. A simple thermoelectric device based on inorganic/organic composite thin film for energy harvesting. *Chem. Eng. J.* **2017**, *320*, 201-10. DOI
173. Li, Z.; Sun, H.; Hsiao, C.; et al. A free-standing high-output power density thermoelectric device based on structure-ordered PEDOT:PSS. *Adv. Elect. Materials*. **2018**, *4*, 1700496. DOI
174. Varghese, T.; Hollar, C.; Richardson, J.; et al. High-performance and flexible thermoelectric films by screen printing solution-processed nanoplate crystals. *Sci. Rep.* **2016**, *6*, 33135. DOI PubMed PMC
175. Wang, L.; Zhang, Z.; Geng, L.; et al. Solution-printable fullerene/TiS₂ organic/inorganic hybrids for high-performance flexible n-type thermoelectrics. *Energy. Environ. Sci.* **2018**, *11*, 1307-17. DOI
176. Gao, Z.; Wei, T. R.; Deng, T.; et al. High-throughput screening of 2D van der Waals crystals with plastic deformability. *Nat. Commun.* **2022**, *13*, 7491. DOI PubMed PMC
177. Wei, S.; Zhang, Y.; Lv, H.; Deng, L.; Chen, G. SWCNT network evolution of PEDOT:PSS/SWCNT composites for thermoelectric application. *Chem. Eng. J.* **2022**, *428*, 131137. DOI
178. Thomas, T. H.; Harkin, D. J.; Gillett, A. J.; et al. Short contacts between chains enhancing luminescence quantum yields and carrier mobilities in conjugated copolymers. *Nat. Commun.* **2019**, *10*, 2614. DOI PubMed PMC
179. Venkateshvaran, D.; Nikolka, M.; Sadhanala, A.; et al. Approaching disorder-free transport in high-mobility conjugated polymers. *Nature* **2014**, *515*, 384-8. DOI

180. Yang, K.; Zhang, X.; Harbuzaru, A.; et al. Stable organic diradicals based on fused quinoidal oligothiophene imides with high electrical conductivity. *J. Am. Chem. Soc.* **2020**, *142*, 4329–40. [DOI](#)
181. Zhou, Y.; Wang, Z.; Yao, Z.; et al. Systematic investigation of solution-state aggregation effect on electrical conductivity in doped conjugated polymers. *CCS. Chem.* **2021**, *3*, 2994–3004. [DOI](#)
182. Naab, B. D.; Guo, S.; Olthof, S.; et al. Mechanistic study on the solution-phase n-doping of 1,3-dimethyl-2-aryl-2,3-dihydro-1H-benzimidazole derivatives. *J. Am. Chem. Soc.* **2013**, *135*, 15018–25. [DOI](#) [PubMed](#) [PMC](#)
183. Lu, Y.; Yu, Z. D.; Un, H. I.; et al. Persistent conjugated backbone and disordered lamellar packing impart polymers with efficient n-doping and high conductivities. *Adv. Mater.* **2021**, *33*, e2005946. [DOI](#) [PubMed](#)
184. Lu, Y.; Wang, J. Y.; Pei, J. Achieving efficient n-doping of conjugated polymers by molecular dopants. *Acc. Chem. Res.* **2021**, *54*, 2871–83. [DOI](#)
185. Yu, Z. D.; Lu, Y.; Wang, Z. Y.; et al. High n-type and p-type conductivities and power factors achieved in a single conjugated polymer. *Sci. Adv.* **2023**, *9*, eadf3495. [DOI](#) [PubMed](#) [PMC](#)
186. Yang, C. Y.; Ding, Y. F.; Huang, D.; et al. A thermally activated and highly miscible dopant for n-type organic thermoelectrics. *Nat. Commun.* **2020**, *11*, 3292. [DOI](#) [PubMed](#) [PMC](#)
187. Liu, H.; Yin, X.; Chi, C.; et al. Direct printing of flexible multilayer composite electrodes based on electrohydrodynamic printing. *ACS. Appl. Electron. Mater.* **2024**, *6*, 724–36. [DOI](#)
188. Ding, X.; Liow, C. H.; Zhang, M.; et al. Surface plasmon resonance enhanced light absorption and photothermal therapy in the second near-infrared window. *J. Am. Chem. Soc.* **2014**, *136*, 15684–93. [DOI](#)
189. Wang, J.; Li, Y.; Deng, L.; et al. High-performance photothermal conversion of narrow-bandgap Ti_2O_3 nanoparticles. *Adv. Mater.* **2017**, *29*. [DOI](#) [PubMed](#)
190. Jiang, Y.; Li, J.; Zhen, X.; Xie, C.; Pu, K. Dual-peak absorbing semiconducting copolymer nanoparticles for first and second near-infrared window photothermal therapy: a comparative study. *Adv. Mater.* **2018**, *30*, e1705980. [DOI](#) [PubMed](#)
191. Chen, C.; Li, Y.; Song, J.; et al. Highly flexible and efficient solar steam generation device. *Adv. Mater.* **2017**, *29*. [DOI](#)
192. Jun, Y. S.; Wu, X.; Ghim, D.; Jiang, Q.; Cao, S.; Singamaneni, photothermal membrane water treatment for two worlds. *Acc. Chem. Res.* **2019**, *52*, 1215–25. [DOI](#) [PubMed](#)
193. Yang, M.; Tan, C. F.; Lu, W.; Zeng, K.; Ho, G. W. Spectrum tailored defective 2D semiconductor nanosheets aerogel for full-spectrum-driven photothermal water evaporation and photochemical degradation. *Adv. Funct. Materials.* **2020**, *30*, 2004460. [DOI](#)
194. Zhang, Q.; Huang, A.; Ai, X.; et al. Transparent power-generating windows based on solar-thermal-electric conversion. *Adv. Energy. Mater.* **2021**, *11*, 2101213. [DOI](#)
195. Lu, Y.; Xiao, X.; Fu, J.; et al. Novel smart textile with phase change materials encapsulated core-sheath structure fabricated by coaxial electrospinning. *Chem. Eng. J.* **2019**, *355*, 532–9. [DOI](#)
196. Chang, J.; Shi, L.; Zhang, M.; et al. Tailor-made white photothermal fabrics: a bridge between pragmatism and aesthetic. *Adv. Mater.* **2023**, *35*, e2209215. [DOI](#) [PubMed](#)
197. Zhuo, S.; Jiang, W.; Dong, Z. Y.; et al. Large-area nanofiber membrane of NIR photothermal $\text{Cs}_{0.32}\text{WO}_3$ for flexible and all-weather solar thermoelectric generation. *Chem. Eng. J.* **2024**, *479*, 147571. [DOI](#)
198. Sun, Z.; Hu, Y.; Wei, C.; et al. Transparent, photothermal and stretchable alginate-based hydrogels for remote actuation and human motion sensing. *Carbohydr. Polym.* **2022**, *293*, 119727. [DOI](#)
199. Xiang, D.; Liu, L.; Chen, X.; et al. High-performance fiber strain sensor of carbon nanotube/thermoplastic polyurethane@styrene butadiene styrene with a double percolated structure. *Front. Mater. Sci.* **2022**, *16*, 586. [DOI](#)
200. Xiang, D.; Zhang, X.; Harkin-jones, E.; et al. Synergistic effects of hybrid conductive nanofillers on the performance of 3D printed highly elastic strain sensors. *Compos. Part. A. Appl. Sci. Manuf.* **2020**, *129*, 105730. [DOI](#)
201. Wan, B.; Liu, N.; Zhang, Z.; et al. Water-dispersible and stable polydopamine coated cellulose nanocrystal-MXene composites for high transparent, adhesive and conductive hydrogels. *Carbohydr. Polym.* **2023**, *314*, 120929. [DOI](#)
202. Sun, X.; Liang, Y.; Ye, L.; Liang, H. An extremely tough and ionic conductive natural-polymer-based double network hydrogel. *J. Mater. Chem. B.* **2021**, *9*, 7751–9. [DOI](#)
203. Gao, T.; Li, N.; Yang, Y.; et al. Mechanical reliable, NIR light-induced rapid self-healing hydrogel electrolyte towards flexible zinc-ion hybrid supercapacitors with low-temperature adaptability and long service life. *J. Energy. Chem.* **2024**, *92*, 63–73. [DOI](#)
204. Xue, C.; Xu, X.; Zhang, L.; et al. Self-healing/pH-responsive/inherently antibacterial polysaccharide-based hydrogel for a photothermal strengthened wound dressing. *Colloids. Surf. B. Biointerfaces.* **2022**, *218*, 112738. [DOI](#)
205. Hou, M.; Yu, M.; Liu, W.; et al. Mxene hybrid conductive hydrogels with mechanical flexibility, frost-resistance, photothermoelectric conversion characteristics and their multiple applications in sensing. *Chem. Eng. J.* **2024**, *483*, 149299. [DOI](#)
206. Yang, H.; Li, J.; Xiao, X.; et al. Topographic design in wearable MXene sensors with in-sensor machine learning for full-body avatar reconstruction. *Nat. Commun.* **2022**, *13*, 5311. [DOI](#) [PubMed](#) [PMC](#)
207. Armstrong, L. E.; Casa, D. J.; Belval, L. N. Metabolism, bioenergetics and thermal physiology: influences of the human intestinal microbiota. *Nutr. Res. Rev.* **2019**, *32*, 205–17. [DOI](#) [PubMed](#)
208. Borghini, S.; Tassi, S.; Chiesa, S.; et al. Clinical presentation and pathogenesis of cold-induced autoinflammatory disease in a family with recurrence of an NLRP12 mutation. *Arthritis. Rheum.* **2011**, *63*, 830–9. [DOI](#) [PubMed](#) [PMC](#)
209. Zeng, P.; Bengtsson, C.; Klareskog, L.; Alfredsson, L. Working in cold environment and risk of developing rheumatoid arthritis: results from the Swedish EIRA case-control study. *RMD. Open.* **2017**, *3*, e000488. [DOI](#) [PubMed](#) [PMC](#)

210. Park, C.; Kim, M. S.; Kim, H. H.; et al. Stretchable conductive nanocomposites and their applications in wearable devices. *Appl. Phys. Rev.* **2022**, *9*, 021312. DOI
211. Pang, G.; Yang, G.; Pang, Z. Review of robot skin: a potential enabler for safe collaboration, immersive teleoperation, and affective interaction of future collaborative robots. *IEEE. Trans. Med. Robot. Bionics.* **2021**, *3*, 681-700. DOI
212. Yi, N.; Gao, Y.; Verso, A. L. J.; et al. Fabricating functional circuits on 3D freeform surfaces via intense pulsed light-induced zinc mass transfer. *Mater. Today. (Kidlington).* **2021**, *50*, 24-34. DOI PubMed PMC
213. Chen, A.; Zhang, C.; Zhu, G.; Wang, Z. L. Polymer materials for high-performance triboelectric nanogenerators. *Adv. Sci. (Weinh).* **2020**, *7*, 2000186. DOI PubMed PMC
214. Luo, Y.; Zhao, L.; Luo, G.; et al. All electrospun fabrics based piezoelectric tactile sensor. *Nanotechnology* **2022**, *33*, 415502. DOI
215. Yi, Y.; Wang, B.; Liu, X.; Li, C. Flexible piezoresistive strain sensor based on CNTs-polymer composites: a brief review. *Carbon. Lett.* **2022**, *32*, 713-26. DOI
216. Park, S.; Heo, S. W.; Lee, W.; et al. Self-powered ultra-flexible electronics via nano-grating-patterned organic photovoltaics. *Nature* **2018**, *561*, 516-21. DOI
217. Yang, Y.; Gao, W. Wearable and flexible electronics for continuous molecular monitoring. *Chem. Soc. Rev.* **2019**, *48*, 1465-91. DOI
218. Cao, X.; Xiong, Y.; Sun, J.; Zhu, X.; Sun, Q.; Wang, Z. L. Piezoelectric nanogenerators derived self-powered sensors for multifunctional applications and artificial intelligence. *Adv. Funct. Materials.* **2021**, *31*, 2102983. DOI
219. Zhang, J.; Bai, C.; Wang, Z.; Liu, X.; Li, X.; Cui, X. Low-grade thermal energy harvesting and self-powered sensing based on thermogalvanic hydrogels. *Micromachines. (Basel).* **2023**, *14*, 155. DOI PubMed PMC
220. Liu, Y.; Cui, M.; Ling, W.; et al. Thermo-electrochemical cells for heat to electricity conversion: from mechanisms, materials, strategies to applications. *Energy. Environ. Sci.* **2022**, *15*, 3670-87. DOI
221. Shi, X.; Ma, L.; Li, Y.; et al. Double hydrogen-bonding reinforced high-performance supramolecular hydrogel thermocell for self-powered sensing remote-controlled by light. *Adv. Funct. Materials.* **2023**, *33*, 2211720. DOI
222. Li, X.; Li, J.; Wang, T.; et al. Self-powered respiratory monitoring strategy based on adaptive dual-network thermogalvanic hydrogels. *ACS. Appl. Mater. Interfaces.* **2022**, *14*, 48743-51. DOI
223. Cacicedo, M. L.; Castro, M. C.; Servetas, I.; et al. Progress in bacterial cellulose matrices for biotechnological applications. *Bioresour. Technol.* **2016**, *213*, 172-80. DOI
224. Li, J.; Chen, S.; Han, Z.; et al. High performance bacterial cellulose organogel-based thermoelectrochemical cells by organic solvent-driven crystallization for body heat harvest and self-powered wearable strain sensors. *Adv. Funct. Materials.* **2023**, *33*, 2306509. DOI
225. Zhou, Z.; Chen, K.; Li, X.; et al. Sign-to-speech translation using machine-learning-assisted stretchable sensor arrays. *Nat. Electron.* **2020**, *3*, 571-8. DOI
226. Li, G.; Hu, Y.; Chen, J.; et al. Thermoelectric and photoelectric dual modulated sensors for human internet of things application in accurate fire recognition and warning. *Adv. Funct. Materials.* **2023**, *33*, 2303861. DOI
227. Li, L.; Wang, D.; Zhang, D.; et al. Near-infrared light triggered self-powered mechano-optical communication system using wearable photodetector textile. *Adv. Funct. Materials.* **2021**, *31*, 2104782. DOI
228. Ding, J.; Zhao, W.; Jin, W.; Di, C.; Zhu, D. Advanced thermoelectric materials for flexible cooling application. *Adv. Funct. Materials.* **2021**, *31*, 2010695. DOI
229. Hsu, A. L.; Herring, P. K.; Gabor, N. M.; et al. Graphene-based thermopile for thermal imaging applications. *Nano. Lett.* **2015**, *15*, 7211-6. DOI
230. Gao, F.; Min, P.; Ma, Q.; et al. Multifunctional thermoelectric temperature sensor for noncontact information transfer and tactile sensing in human-machine interaction. *Adv. Funct. Materials.* **2024**, *34*, 2309553. DOI
231. Zakery, A.; Elliott, S. Optical properties and applications of chalcogenide glasses: a review. *J. Non-Cryst. Solids.* **2003**, *330*, 1-12. DOI
232. Fu, Y.; Kang, S.; Xiang, G.; et al. Ultraflexible temperature-strain dual-sensor based on chalcogenide glass-polymer film for human-machine interaction. *Adv. Mater.* **2024**, *36*, e2313101. DOI PubMed
233. Wang, W.; Jiang, Y.; Zhong, D.; et al. Neuromorphic sensorimotor loop embodied by monolithically integrated, low-voltage, soft e-skin. *Science* **2023**, *380*, 735-42. DOI
234. Jung, D.; Lim, C.; Shim, H. J.; et al. Highly conductive and elastic nanomembrane for skin electronics. *Science* **2021**, *373*, 1022-6. DOI
235. Chen, C.; Xu, J. L.; Wang, Q.; et al. Biomimetic multimodal receptors for comprehensive artificial human somatosensory system. *Adv. Mater.* **2024**, *36*, e2313228. DOI
236. Chen, C.; Xu, F. Q.; Wu, Y.; et al. Manipulating hetero-nanowire films for flexible and multifunctional thermoelectric devices. *Adv. Mater.* **2024**, *36*, e2400020. DOI PubMed